Mean-field theory for interchain orientational ordering of conjugated polymers

Han-Yong Choi, A. B. Harris, and E. J. Mele
Department of Physics, University of Pennsylvania, Philadelphia, Pennsylvania 19104-6396
(Received 3 April 1989)

We consider a generalized anisotropic planar-rotor model on a triangular lattice for interchain orientational ordering of undoped and doped polyacetylene, and investigate the effects of various terms on the symmetry and the range of stability of the observed herringbone (HB) phases. Dipole, quadrupole, and octopole interactions are included in the model with sixfold crystal-field anisotropy and are analyzed within the mean-field theory. The relative strength of these interactions can be estimated from the observed setting angle of the HB phase with the help of the smallness of crystal-field anisotropy. A model where the polymer chain is represented by a "quadrupolar" mass density only has various phases as the temperature and the interaction parameters are varied. Among them, the HB phase is found below a critical temperature T_c for some range of the parameter space, and the setting angle of the HB phase is 45° and independent of temperature. Competition between quadrupole and other interactions such as dipole or octopole, parametrized by the ratio of interaction strengths λ, results in an additional phase transition at $T_c'(\lambda)$ and makes the setting angle vary with the temperature below $T_c'(\lambda)$. For a model with quadrupole and octopole terms, there are two degenerate states of the setting angle related by $\theta' = \pi/2 - \theta$. This degeneracy does not reflect a symmetry of the system and is lifted by the dipole terms. For a model with quadrupole and dipole interactions, the setting angle increases as the temperature is reduced below $T_c'(\lambda)$. From these results, we conclude that quadrupole and dipole interactions are important terms to explain experimental observations. Effects of crystal-field anisotropy resolve the twofold degeneracy, destroy the critical behavior associated with $T_c'(\lambda)$, and make the setting angle temperature dependent over the entire range of temperature below T_c. Crucial information on the interaction parameters of the model can be obtained through the temperature dependence of the setting angle of the HB phase.

I. INTRODUCTION

Doping of conducting polymers involves charge transfer to π-electron manifolds and the insertion of counter ions between polymer chains. As a result, the doping process induces considerable perturbation of the crystal structure of the pristine polymer, and leads to the formation of a new ordered structure depending on the degree of crystallinity of the starting polymer and the size of the counter ion. Identification of the structure of these phases induced by doping is of fundamental importance, because electronic properties are determined by the structure. Shacklette and Toth[1] reported experiments with x-ray and electrochemical measurements suggesting that ion insertion during doping proceeds, not at random, but via a sequence of crystalline phases. Recently, Winokur *et al.*[2] carried out an x-ray scattering experiment on sodium-doped polyacetylene. They observed that the sodium ions form a $\sqrt{3}\times\sqrt{3}$ superstructure with respect to the triangular lattice of $(CH)_x$ chains at the critical chemical potential for the dopants μ_c, and discommensurate domain-wall phase for a small range of chemical potential below μ_c. Structural properties of undoped $(CH)_x$ also have been studied intensely.[3] The space group of *trans*-$(CH)_x$ was determined to be $P2_1/n$. Polymer chains form a herringbone (HB) structure on a pseudotriangular lattice,[3,4] and the setting angle of the HB phase[4] with respect to [100] was found to be about 55°, as shown in Fig. 1.

The analogous problem in one dimension has been studied intensively over the last decade; that is, the problem of intercalated graphites,[5] which involves formation of an ordered one-dimensional (1D) superlattice of occupied and empty galleries with variable 2D in-plane density in the occupied ones. A simple Ising-type model[6] has

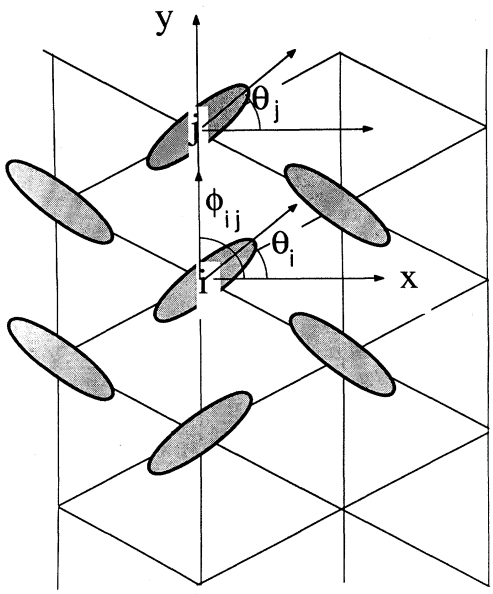

FIG. 1. Schematic diagram of $(CH)_x$ structure projected along the chain direction. Polymer chain indexed by i is represented by a rotor on a two-dimensional triangular lattice, with the setting angle θ_i with respect to x axis.

been quite successful in analyzing and guiding experiments. One obvious line of approach to the problem of interchain ordering of polymers will be the extension of the same kind of model employed in the intercalated graphites to two dimensions.[7] In this approach, one needs to determine the effective interaction between polymer chains considering both the density modulations and the angular displacements. The increase of dimensionality makes polymer problems more complicated and interesting, because there are angular degrees of freedom in addition to the translational ones. As a preliminary step for investigating doping-induced structural transformations, we study a generalized-anisotropic-planar-rotor (GAPR) model to identify appropriate interactions to model the interchain ordering of $(CH)_x$. Work on the structural phase transition induced by doping will be reported in a separate paper.[8] A similar but simpler model was studied by Harris *et al.*[9] as a model for homopolar diatomic molecules such as H_2, D_2, and N_2 adsorbed on a graphite surface. Mean-field analyses employed in this work are similar to their formulation of the problem.

In Sec. II, we will introduce the GAPR model on a triangular lattice for the interchain ordering of undoped $(CH)_x$. Mean-field theory will be developed in Sec. III, to obtain the phase diagram of the model and to study the symmetry of the HB phase. Results of our calculations with emphasis on the temperature dependence of the setting angle will also be given. We will present arguments indicating the smallness of the crystal-field anisotropy and favoring a model with quadrupole and dipole interactions. In Sec. IV, we will study the spin-wave spectrum of rotors to investigate the range of stability of the HB phase. Section V contains the summary of our analyses and concluding remarks. In the Appendixes, a Landau expansion for the model we consider and analyses for a $\sqrt{3}\times\sqrt{3}$ ordering transition and other calculational details will be given.

II. MODEL HAMILTONIAN

We are primarily interested in the interchain orientational ordering of the undoped polyacetylene on a two-dimensional triangular lattice as a preliminary step toward a study of the dopant ordering in the process of electrochemical doping. For this purpose, the polymer structure is projected along the chain direction and each polymer chain is represented by a "rotor" on a two-dimensional triangular lattice. We assume that we can separate the deformation energies associated with the angular displacements and translational ones; that is, we assume the orientational degrees of freedom are the soft degrees of freedom compared with translational ones. The fact that we treat this problem in two dimensions can be justified on the grounds that the ordering-induced strain energy favors aggregation of dopants into columns (directed along the chain axis),[10] which is the same physical argument that was adopted in the staging Hamiltonian in the problem of intercalated graphite.[5,6]

The mass distribution of the rotor which models the polymer chain will be decomposed into various angular momentum channels. We will include $m=0$, 1, 2, and 3 components, which represent "monopole," "dipole," "quadrupole," and "octopole" moments of the mass distribution. Relative strength among these terms has not been estimated from a more microscopic theory. However, as we will see in Sec. III, the information on the relative strength of these terms can be obtained from the temperature dependence on the setting angle of the HB phase. Because the $(CH)_x$ chain is not symmetric under the rotation by π about an axis parallel to the chain axis, the dipole moment will not vanish in general. In fact, as shown in Sec. III D, the dipole interaction is found to be essential to explain the experimental observation of the HB phase-setting angle. The quadrupole moment in two dimensions is represented by

$$Q_{xx}(\theta_j)=a\cos(2\theta_j)\ ,$$

$$Q_{yy}(\theta_j)=-a\cos(2\theta_j)\ ,$$

and

$$Q_{xy}(\theta_j)=Q_{yx}(\theta_j)=a\sin(2\theta_j)\ ,$$

where θ_j is the angular displacement of the jth rotor with respect to the x axis, and a is the magnitude of the quadrupole moment determined by the mass distribution. Invariant forms for the interaction between quadrupole moments are

$$\sum_{k,l} Q_{kl}(\theta_i)Q_{kl}(\theta_j)\ ,$$

$$\sum_{k,l,m,n} Q_{kl}(\theta_i)Q_{mn}(\theta_j)x_k(i,j)x_l(i,j)x_m(i,j)x_n(i,j)\ ,$$

and

$$\sum_{k,l,m} Q_{kl}(\theta_i)Q_{lm}(\theta_j)x_k(i,j)x_m(i,j)\ ,$$

where $x_k(i,j)$ is the kth component of a vector connecting the ith and jth rotors. The above three forms can be reduced to linear combinations of $\cos(2\theta_i-2\theta_j)$ and

$$\cos(2\theta_i-2\phi_{ij})\cos(2\theta_j-2\phi_{ij})\ ,$$

with

$$\mathbf{x}(ij)=\begin{bmatrix}\cos\phi_{ij}\\ \sin\phi_{ij}\end{bmatrix}\ .$$

From the above analyses we take the following model for the interactions between rotors,

$$H_2=\alpha\sum_{\langle i,j\rangle}\cos(2\theta_i-2\theta_j)+\beta\sum_{\langle i,j\rangle}\cos(2\theta_i-2\phi_{ij})\cos(2\theta_j-2\phi_{ij})\ , \tag{1}$$

where the summation is over nearest neighbors, and α and β are interaction parameters to be estimated. For the second term, ϕ_{ij}, the angle of a vector connecting ith and jth rotors, is determined by the geometry of the underlying lattice, and this term represents the anisotropic part of the interactions between rotors. For electrostatic interactions between quadrupoles, it is easy to show that $\beta/\alpha=-\frac{35}{16}$ and $\alpha<0$. Interaction between dipoles can be written in the same form as Eq. (1),

$$H_1=\alpha_1\sum_{\langle i,j\rangle}\cos(\theta_i-\theta_j)$$
$$+\beta_1\sum_{\langle i,j\rangle}\cos(\theta_i-\phi_{ij})\cos(\theta_j-\phi_{ij})\ , \tag{2}$$

where $\beta_1/\alpha_1=-3$ and $\alpha_1>0$ for electrostatic interactions between dipoles. We will also consider

$$H_4=\alpha_4\sum_{\langle i,j\rangle}\cos(4\theta_i-4\theta_j)$$
$$+\beta_4\sum_{\langle i,j\rangle}\cos(4\theta_i-4\phi_{ij})\cos(4\theta_j-4\phi_{ij})\ . \tag{3}$$

When $\alpha=-\beta/2$, Eq. (1) is reduced to

$$H=\frac{\beta}{2}\sum_{\langle i,j\rangle}\cos(2\theta_i+2\theta_j-4\phi_{ij})\ ,$$

which was referred to as the anisotropic planar-rotor model and studied by several groups.[9,10] Finally, we consider a sixfold crystal field of the following form:

$$\sum_j V_3\cos(6\theta_j)\ . \tag{4}$$

This form of the field will be due to the interactions between a quadrupole moment and mass densities (monopoles) of surrounding rotors, as is discussed in Sec. III B. We will perform explicit calculations for a model with quadrupole and octopole interactions, which we will refer to as the 2-4 model, for which the orientational energy is given by

$$H_{2\text{-}4}=H_2+H_4\ . \tag{5}$$

We will set $\alpha_4=\lambda\alpha$ and $\beta_4=\lambda\beta$, to reduce the number of parameters. A model with quadrupole and dipole interactions, the 2-1 model, will also be analyzed, for which the orientational energy is given by

$$H_{2\text{-}1}=H_2+H_1 \tag{6}$$

with $\alpha_1=\lambda\alpha$ and $\beta_1=\lambda\beta$.

Mean-field theory will be developed in the following section for several models introduced previously. We will study the mean-field phase diagram, the ground-state energy and orientational structure of the ordered phases, and the spin-wave spectrum of rotors for various of these models. In particular, we will study the phase diagram of the 2 model, which contains quadrupole interactions only, as a function of α and β, the symmetry of the herringbone phases of the 2-4 and 2-1 models, effects of sixfold crystal-field anisotropy, and the spin-wave spectrum of the 2-4 model as a function of λ. To make the presentation more transparent, we list the analyses we carried out for each model in Table I.

A few words are in order about the wave vectors needed to describe the various ordered phases. We take the translation vectors of the triangular lattice as

$$\mathbf{b}_1=a\hat{\mathbf{j}},\quad \mathbf{b}_2=\tfrac{1}{2}a(\sqrt{3}\hat{\mathbf{i}}+\hat{\mathbf{j}})\ , \tag{7}$$

where $\hat{\mathbf{i}}$ and $\hat{\mathbf{j}}$ are unit vectors along the crystal x and y axes, respectively. Correspondingly, we have the basis vectors of the reciprocal lattice as

$$\mathbf{G}_1=[2\pi/(\sqrt{3}a)](\hat{\mathbf{i}}-\sqrt{3}\hat{j}),\quad \mathbf{G}_2=4\pi/(\sqrt{3}a)\hat{\mathbf{i}}\ . \tag{8}$$

These vectors obey $\mathbf{b}_i\cdot\mathbf{G}_j=2\pi\delta_{i,j}$. Note that the HB structure in which columns (parallel to $\hat{\mathbf{j}}$) of rotors assume alternately different angles is described by the

TABLE I. List of analyses for each model.

Model	Hamiltonian	Analyses
2	Quadrupole interactions given by Eq. (1)	Landau expansion; Sec. III A Landau expansion for 33 phase; Appendix B
	Quadrupole interactions with crystal-field anisotropy given by Eq. (28)	Landau expansion; Sec. III B Mean-field theory; Sec. III B
2-4	Quadrupole and octopole interactions given by Eq. (5)	Landau expansion; Appendix A Mean-field theory; Sec. III C Spin-wave spectrum; Sec. IV
	Quadrupole and octopole with crystal-field anisotropy given by Eqs. (5) and (4)	Mean-field theory; Sec. III C
2-1	Quadrupole and dipole interactions given by Eq. (6)	Mean-field theory; Sec. III D
	Quadrupole and dipole with crystal-field anisotropy given by Eqs. (6) and (4)	Mean-field theory; Sec. III D

modulation vector

$$\mathbf{Q}_A=\tfrac{1}{2}\mathbf{G}_2 \ . \tag{9a}$$

Equivalent states rotated by $\pm 2\pi/3$ have modulation vectors

$$\mathbf{Q}_B=\tfrac{1}{2}\mathbf{G}_1 \ , \tag{9b}$$

$$\mathbf{Q}_C=-\mathbf{Q}_A-\mathbf{Q}_B \ . \tag{9c}$$

Apart from a uniform state with wave vector $\mathbf{q}=\mathbf{0}$, one also expects the possible existence of the so-called $\sqrt{3}\times\sqrt{3}$ structure described by the wave vectors $\mathbf{Q}_{\sqrt{3}}$ at a vertex of the first Brillouin zone and $-\mathbf{Q}_{\sqrt{3}}$, where

$$\mathbf{Q}_{\sqrt{3}}=[4\pi/(3a)]\hat{\mathbf{j}}=(2\mathbf{G}_1+\mathbf{G}_2)/3 \ . \tag{9d}$$

Note the difference in the wave vectors for these two structures: for the herringbone case $\mathbf{Q}_A$ and $-\mathbf{Q}_A$ differ by a reciprocal-lattice vector, so in sums over the Brillouin zone only one of this pair is included, and similarly for $\mathbf{Q}_B$ and $\mathbf{Q}_C$. In contrast, $\mathbf{Q}_{\sqrt{3}}$ and $-\mathbf{Q}_{\sqrt{3}}$ do not differ by a reciprocal-lattice vector, so in sums over the Brillouin zone both values should appear separately.

III. MEAN-FIELD THEORY

We will develop a mean-field theory for the free energy per rotor, F, for these models using the ansatz

$$F=\frac{1}{N}\mathrm{Tr}\{\rho H+T\rho\ln\rho\}\equiv U-TS \ , \tag{10}$$

where N is the total number of rotors, the Boltzmann constant k has been set equal to unity, and Tr indicates an integration over all angular coordinates θ_i. Equation (10) is exact if ρ is minimized with respect to all normalized ρ's. In the mean-field approximation the density matrix ρ is taken to be the product of single-rotor density matrices ρ_i of the form

$$\rho_i(\theta_i)=\frac{1}{Z_i}\exp\left[\sum_{m=1}^{\infty}C_i(m)\cos(m\theta_i)+S_i(m)\sin(m\theta_i)\right] , \tag{11}$$

where

$$Z_i=\mathrm{Tr}\left\{\exp\left[\sum_{m=1}^{\infty}C_i(m)\cos(m\theta_i)+S_i(m)\sin(m\theta_i)\right]\right\} .$$

Here we introduce the order parameters $C_i(m)$ and $S_i(m)$, which are allowed to depend on the site index i. We assume that quadrupole interactions are dominant, so that the dominant order parameters are $C_i(2)$ and $S_i(2)$. We will also investigate the appearance of a phase in which order parameters for other m values are important. Average values of $\cos(m\theta_i)$ and $\sin(m\theta_i)$ are obtained by

$$\langle\cos(m\theta_i)\rangle=\partial\ln Z_i/\partial C_i(m) \tag{12a}$$

and

$$\langle\sin(m\theta_i)\rangle=\partial\ln Z_i/\partial S_i(m) \ . \tag{12b}$$

The internal energy per rotor, U, is given by

$$U=\frac{1}{N}\sum_i U_i \quad \text{with } U_i=\mathrm{Tr}(\rho H_i)=\tfrac{1}{2}\sum_j\langle H_{ij}(\theta_i,\theta_j)\rangle \ , \tag{13}$$

where $H_{ij}(\theta_i,\theta_j)$ is the pair interaction of Eqs. (1), (2), or (3), as is appropriate, and $\langle\cdots\rangle$ indicates a thermal average. The free energy is then

$$F=\frac{1}{N}\sum_i F_i$$

$$\text{with } F_i=U_i+T\sum_{m=1}^{\infty}[C_i(m)\langle\cos(m\theta_i)\rangle+S_i(m)\langle\sin(m\theta_i)\rangle-\ln Z_i] \ . \tag{14}$$

By minimizing the free energy given by Eq. (14) with respect to $\langle\cos(m\theta_i)\rangle$ and $\langle\sin(m\theta_i)\rangle$, self-consistency relations are obtained as follows:

$$C_{i(m)}=-T^{-1}\partial U_i/\partial\langle\cos(m\theta_i)\rangle \tag{15a}$$

and

$$S_i(m)=-T^{-1}\partial U_i/\partial\langle\sin(m\theta_i)\rangle \ . \tag{15b}$$

As shown in Sec. III B, $\langle\cos(m\theta_i)\rangle$ and $\langle\sin(m\theta_i)\rangle$ can be eliminated in analytic calculations with the help of Eqs. (12), and the free energy is expressed in terms of independent parameters $C_i(m)$ and $S_i(m)$. In numerical calculations, however, it is much easier to treat $\langle\cos(m\theta_i)\rangle$ and $\langle\sin(m\theta_i)\rangle$ as independent parameters and obtain $C_i(m)$ and $S_i(m)$ in terms of $\langle\cos(m\theta_i)\rangle$ and $\langle\sin(m\theta_i)\rangle$. In other words, we take an arbitrary initial configuration for $C_i(m)$ and $S_i(m)$, which we use in the density matrices, and calculate $\langle\cos(m\theta_i)\rangle$ and $\langle\sin(m\theta_i)\rangle$, by Eq. (12). We then update $C_i(m)$ and $S_i(m)$ in terms of newly calculated $\langle\cos(m\theta_i)\rangle$ and $\langle\sin(m\theta_i)\rangle$ through the self-consistency relations of Eqs. (15a) and (15b), and repeat the previous procedures until self-consistency is obtained. In this work, the parameters in the model are chosen in favor of the HB phase, and the self-consistency equations are solved by numerical iteration as explained. Whether other phases have lower free energy than the HB phase has been checked (a) by calculating the free energy with a 2×2 unit cell at finite temperature, (b) by calculating the ground-state energy at zero temperature with a 4×2 unit cell, and (c) by Landau expansion near the critical temperature as shown in Appendix A. The greatest advantage of Landau expansion is the fact that we do not have to assume periodicity of unit cell, but its disadvantage is that it is only reliable close to the critical region where the order parameters are small.

The Landau expansion can be formulated by expanding the single-density matrices in powers of order parameters. Then Eq. (11) reduces to

$$\rho_i(\theta_i)=\frac{1}{2\pi}\left[1+\sum_{m=1}^{\infty} C_i(m)\cos(m\theta_i) + S_i(m)\sin(m\theta_i)\right] . \tag{16}$$

Then using Eq. (16) it is easy to show that

$$\langle \cos(l\theta_i)\rangle \equiv \mathrm{Tr}\{\cos(l\theta_i)\rho_i\}=\tfrac{1}{2}C_i(l) , \tag{17a}$$

$$\langle \sin(l\theta_i)\rangle \equiv \mathrm{Tr}\{\sin(l\theta_i)\rho_i\}=\tfrac{1}{2}S_i(l) . \tag{17b}$$

If we write $\rho_i(\theta_i)=(1+\delta\rho_i)/2\pi$, then to quadratic order in $\delta\rho_i$ the entropy per rotor is

$$-S\equiv\frac{1}{N}\sum_i \mathrm{Tr}\{\rho_i(\theta_i)\ln\rho_i(\theta_i)\}$$

$$=-S_0+\frac{1}{2N}\sum_i \mathrm{Tr}(\delta\rho_i)^2 \tag{18a}$$

$$=-S_0+\frac{1}{4N}\sum_i\sum_{m=1}\{[C_i(m)]^2+[S_i(m)]^2\} . \tag{18b}$$

The internal energy per rotor, U, in terms of the order parameters is obtained by substituting Eq. (17) into Eq. (13). Thus apart from a constant, the free energy per rotor is given as a quadratic form in the order parameters. We then Fourier transform the order parameters as

$$C_m(\mathbf{q})=\frac{1}{N}\sum_i C_i(m)e^{i\mathbf{q}\cdot\mathbf{r}} \tag{19}$$

and similarly for $S_m(\mathbf{q})$, and obtain the free energy per rotor in momentum space in the following form:

$$F=\tfrac{1}{2}\sum_{\mathbf{q}}\sum_{l,m=1}^{\infty}[\Gamma^{(cc)}_{l,m}(\mathbf{q})C_l(\mathbf{q})C_m(-\mathbf{q})+\Gamma^{(cs)}_{l,m}(\mathbf{q})C_l(\mathbf{q})S_m(-\mathbf{q})+\Gamma^{(sc)}_{l,m}(\mathbf{q})S_l(\mathbf{q})C_m(-\mathbf{q})+\Gamma^{(ss)}_{l,m}(\mathbf{q})S_l(\mathbf{q})S_m(-\mathbf{q})] . \tag{20}$$

For a rather general interaction given by

$$H=\tfrac{1}{2}\sum_{i,j}H_{ij}(\theta_i,\theta_j) ,$$

where

$$H(\theta_i,\theta_j)=\sum_{l,m=1}^{\infty}\{A_{ij}^{(l,m)}\cos[l(\theta_i-\phi_{ij})]\cos[m(\theta_j-\phi_{ij})]+B_{ij}^{(l,m)}\sin[l(\theta_i-\phi_{ij})]\sin[m(\theta_j-\phi_{ij})]\} , \tag{21}$$

we have the following explicit expressions for the Γ's:

$$\Gamma^{(cc)}_{l,m}(\mathbf{q})=\tfrac{1}{2}T\delta_{l,m}+\tfrac{1}{4}\sum_{\mathbf{r}}[A_{\mathbf{r}}^{(l,m)}\cos(l\phi_{\mathbf{r}})\cos(m\phi_{\mathbf{r}})+B_{\mathbf{r}}^{(l,m)}\sin(l\phi_{\mathbf{r}})\sin(m\phi_{\mathbf{r}})]e^{-i\mathbf{q}\cdot\mathbf{r}} \tag{22a}$$

$$\Gamma^{(cs)}_{l,m}(\mathbf{q})=\tfrac{1}{4}\sum_{\mathbf{r}}[A_{\mathbf{r}}^{(l,m)}\cos(l\phi_{\mathbf{r}})\sin(m\phi_{\mathbf{r}})-B_{\mathbf{r}}^{(l,m)}\sin(l\phi_{\mathbf{r}})\cos(m\phi_{\mathbf{r}})]e^{-i\mathbf{q}\cdot\mathbf{r}} , \tag{22b}$$

$$\Gamma^{(sc)}_{l,m}(\mathbf{q})=\tfrac{1}{4}\sum_{\mathbf{r}}[A_{\mathbf{r}}^{(l,m)}\sin(l\phi_{\mathbf{r}})\cos(m\phi_{\mathbf{r}})-B_{\mathbf{r}}^{(l,m)}\cos(l\phi_{\mathbf{r}})\sin(m\phi_{\mathbf{r}})]e^{-i\mathbf{q}\cdot\mathbf{r}} , \tag{22c}$$

$$\Gamma^{(ss)}_{l,m}(\mathbf{q})=\tfrac{1}{2}T\delta_{l,m}+\tfrac{1}{4}\sum_{\mathbf{r}}[A_{\mathbf{r}}^{(l,m)}\sin(l\phi_{\mathbf{r}})\sin(m\phi_{\mathbf{r}})+B_{\mathbf{r}}^{(l,m)}\cos(l\phi_{\mathbf{r}})\cos(m\phi_{\mathbf{r}})]e^{-i\mathbf{q}\cdot\mathbf{r}} , \tag{22d}$$

where $A_{\mathbf{r}}^{(l,m)}\equiv A_{ij}^{(l,m)}$ with $\mathbf{r}=\mathbf{r}_i-\mathbf{r}_j$ and similarly with other subscripted variables. Γ's are the elements of the inverse susceptibility matrix in the space spanned by the $C_m(\mathbf{q})$'s and $S_m(\mathbf{q})$'s. There are now two possibilities; one has either a first-order or a second-order phase transition. We have to go to higher order in the Landau expansion to tell which one of the two in fact occurs. Positive fourth-order terms without third-order ones most likely indicate that a second-order phase transition occurs. Otherwise the transition is a first-order one. If it is second order, we can locate the wave vector which describes the period of ordered phase, critical variables, and transition temperature by finding zeros of the inverse susceptibility matrix, the elements of which are Γ's given by Eqs. (22). These expressions will be used later for the Landau expansion.

In Sec. III A we will study the 2 model, which includes only the quadrupole interactions given by Eq. (1), as a function of α, β, and temperature. The HB phase is found in some range of the parameter space, and is associated with critical fluctuations in $\langle \sin(2\theta)\rangle$. Because of the dominance of the criticality of $\langle \sin(2\theta_i)\rangle$, the symmetry of this critical point is such that the setting angle of the HB phase is always 45° in the absence of single-rotor anisotropy, a value which is inconsistent with the experimental observations.[4] In the following sections, therefore, we will consider other interactions to obtain the HB phase with the observed setting angle of about 55°. There are several possibilities of obtaining 55° HB phase. Among them, one simple way is to use sixfold crystal-field anisotropy (Sec. III B), which favors the orientation along the bond direction (HB setting angle of

30° with respect to the x axis in the notation of Fig. 1), or favors a setting angle of 60°. This kind of anisotropy, as shown in Sec. III B, is due to the interaction between a quadrupole moment and surrounding mass densities (monopole moments). Because of the smallness of V_3, however, it is not likely that the 55° HB phase is due to the crystal-field anisotropy. Another way of obtaining a HB phase where the setting angle is different from 45° is to include other interactions with different angular dependence. For example, we consider both octopole and dipole interactions. The motivation is that through the competition between quadrupole and octopole (or dipole) interactions we may be able to obtain a HB phase with a 55° setting angle. We will therefore consider octopole (Sec. III C) and dipole (Sec. III D) interactions in addition to the quadrupole one.

A. Phase diagram for the 2 model

In this subsection we will investigate the phase diagram of the 2 model for which the Hamiltonian is given by Eq. (1), as a function of α and β. To do this we start by analyzing the instabilities within Landau theory that one encounters as the temperature is reduced. The wave vector at which an instability first occurs indicates the nature of the ordered phase, assuming that a discontinuous transition does not intervene. Then we will determine the ground state as a function of the coupling constants. By integrating the results of these analyses, we will draw a tentative phase diagram in the T-β plane both for $\alpha=1$ and for $\alpha=-1$, which without considering the anisotropic part will favor the ferromagnetic and $\sqrt{3}\times\sqrt{3}$ phase, respectively. These results will also indicate interesting regions of these phase diagrams for numerical study. In particular, a provocative result is the existence of a longitudinally modulated phase with an incommensurate wave vector.

We start with an analysis of the instabilities within Landau theory. As in Eqs. (22) we have

$$\Gamma_{2,2}^{(cc)}(\mathbf{q})=\tfrac{1}{2}T+\tfrac{1}{2}\alpha(\gamma_1+\gamma_2+\gamma_3)+\tfrac{1}{2}\beta(\gamma_1+\tfrac{1}{4}\gamma_2+\tfrac{1}{4}\gamma_3)\ , \tag{23a}$$

$$\Gamma_{2,2}^{(cs)}(\mathbf{q})=\Gamma_{2,2}^{(sc)}(\mathbf{q})=\tfrac{1}{8}\beta\sqrt{3}(\gamma_2-\gamma_3)\ , \tag{23b}$$

$$\Gamma_{2,2}^{(ss)}(\mathbf{q})=\tfrac{1}{2}T+\tfrac{1}{2}\alpha(\gamma_1+\gamma_2+\gamma_3)+\tfrac{3}{8}\beta(\gamma_2+\gamma_3)\ , \tag{23c}$$

where $\gamma_i=\cos(\mathbf{q}\cdot\boldsymbol{\delta}_i)$ and $\boldsymbol{\delta}_i$ is the ith nearest-neighbor vector: $\boldsymbol{\delta}_1=a\hat{\mathbf{j}}$, $\boldsymbol{\delta}_2=\frac{1}{2}a(\sqrt{3}\hat{\mathbf{i}}+\hat{\mathbf{j}})$, and $\boldsymbol{\delta}_3=\frac{1}{2}a(\sqrt{3}\hat{\mathbf{i}}-\hat{\mathbf{j}})$. From the eigenvalues of the inverse susceptibility matrix $\Gamma_{2,2}$, the elements of which are given in Eqs. (23), we find that the transition temperature corresponds to the maximum (with respect to choice of $\mathbf{q}$ and choice of sign) of

$$\lambda_\pm=-(\alpha+\tfrac{1}{2}\beta)(\gamma_1+\gamma_2+\gamma_3)\pm\tfrac{1}{2}\beta(\gamma_1^2+\gamma_2^2+\gamma_3^2-\gamma_1\gamma_2-\gamma_2\gamma_3-\gamma_3\gamma_1)^{1/2}\ . \tag{24}$$

If one discounts the possibility of solutions other than those corresponding to the zone center, the herringbone vectors, or the $\sqrt{3}\times\sqrt{3}$ phase, then one can take the maximum over the solutions

$$T_{\mathrm{FM}}=-3\alpha-\tfrac{3}{2}\beta\ , \tag{25a}$$

$$T_{\mathrm{HB},s}=\alpha+\tfrac{3}{2}\beta\ , \tag{25b}$$

$$T_{\mathrm{HB},c}=\alpha-\tfrac{1}{2}\beta\ , \tag{25c}$$

$$T_{\sqrt{3}}=\tfrac{3}{2}\alpha+\tfrac{3}{4}\beta\ . \tag{25d}$$

Here FM denotes ferromagnetic ($\mathbf{q}=\mathbf{0}$), HB,s the herringbone phase with order parameter $\langle\sin2\theta\rangle$, HB,$c$ the herringbone phase with order parameter $\langle\cos2\theta\rangle$, and $\sqrt{3}$ the so-called $\sqrt{3}\times\sqrt{3}$ structure, with modulation vector $\mathbf{Q}_{\sqrt{3}}$ at a vertex of the Brillouin zone given by Eq. (9d). From Eqs. (25) one finds that each of these phases has a regime of a stability as follows:

FM: $\beta<-(4\alpha/3)$ and $\beta<-4\alpha$, $T_c=-3\alpha-\frac{3}{2}\beta$, (26a)

HB,c: $\beta<-(2\alpha/5)$ and $\beta>-4\alpha$, $T_c=\alpha-\frac{1}{2}\beta$, (26b)

HB,s: $\beta>-(4\alpha/3)$ and $\beta>(2\alpha/3)$, $T_c=\alpha+\frac{3}{2}\beta$, (26c)

$\sqrt{3}$: $\beta<2\alpha/3$ and $\beta>-(2\alpha/5)$, $T_c=\frac{3}{2}\alpha+\frac{3}{4}\beta$. (26d)

Actually, we have carried out a search throughout the zone to check whether the instability does, in fact, occur at one of the above-listed symmetry points. By maximizing $\lambda_\pm$ of Eq. (24) we find that for α positive and $0<\beta<\frac{4}{3}\alpha$ an incommensurate state appears. Thus Eq. (26) should be revised: Eqs. (26a) and (26b) remain but the other regimes are

HB,s: $\beta>-(4\alpha/3)$ and $\beta>4\alpha/3$, $T_c=\alpha+\frac{3}{2}\beta$, (26c′)

$\sqrt{3}$: $\beta<0$ and $\beta>-(2\alpha/5)$, $T_c=\frac{3}{2}\alpha+\frac{3}{4}\beta$, (26d′)

mod: $\beta>0$ and $\beta<4\alpha/3$, $T_c=\frac{3}{2}\alpha+\frac{3}{4}\beta+\frac{9}{32}\beta^2/\alpha$, (26e)

where mod refers to a modulated phase whose wave vector is given by

$$q_x=2\pi/\sqrt{3}a,\quad \cos(\tfrac{1}{2}aq_y)=(4\alpha+3\beta)/8\alpha\ . \tag{27}$$

For $\beta=0$, $\mathbf{q}$ describes the $\sqrt{3}\times\sqrt{3}$ state, whereas for $\beta=4\alpha/3$, $\mathbf{q}=\hat{\mathbf{i}}2\pi/\sqrt{3}a$ describes the herringbone phase. In this modulated phase, there is still an instability in $\Gamma_{2,2}^{(ss)}$, but the wave vector is no longer that of the herringbone phase. So it has an amplitude modulation of the order parameter. This needs further study. Results summarized in Eqs. (26) are shown in Fig. 2. DS represents disordered phase and other notations are the same as in Eqs. (26). Figure (2a) is for $\alpha>0$ and 2(b) is for $\alpha<0$. Note that only FM and HB,s phases appear for $\alpha<0$.

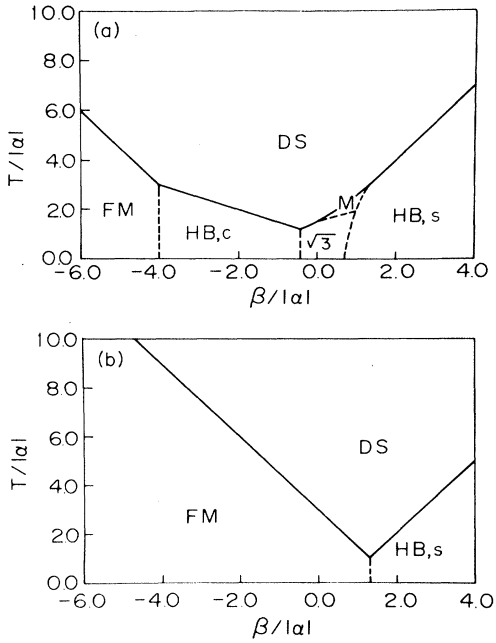

FIG. 2. Phase diagram of the 2 model in the T-β plane. (a) is for $\alpha=1$ and (b) is for $\alpha=-1$. DS, FM, $\sqrt{3}$, M, and HB represent disordered, ferromagnetic, $\sqrt{3}\times\sqrt{3}$, modulated, and herringbone phases, respectively. Subscript c and s for the HB phase means that $\cos(2\theta)$ and $\sin(2\theta)$ become critical first as temperature is reduced, respectively. Solid lines represent the second-order transition and dashed lines the first-order one. See Appendix B for the details about the phase transition of the $\sqrt{3}\times\sqrt{3}$ phase.

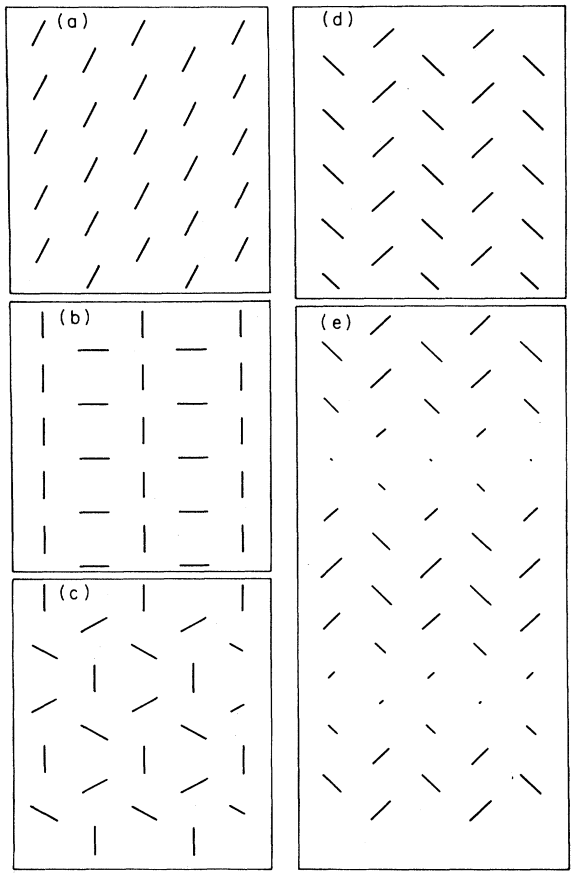

FIG. 3. Configurations of the phases occurring in Fig. 2. (a)–(e) represent FM, HB,c, $\sqrt{3}\times\sqrt{3}$, HB,s, and mod phases, respectively. FM and $\sqrt{3}\times\sqrt{3}$ phases are invariant under the global spin rotation. Note the longitudinal nature of the modulation in the mod phase. The length of a rotor at a site is proportional to the amplitude of order parameter at the site.

The configuration of each phase of Fig. 2 is shown in Fig. 3. Panels (a), (b), (c), (d), and (e) represent FM, HB,c, $\sqrt{3}$, HB,s and mod phases, respectively. FM and $\sqrt{3}$ phases are invariant with respect to the global spin rotation. Note the longitudinal nature of modulation of the mod phase. As is analyzed with Landau expansion in Appendix B, the $\sqrt{3}\times\sqrt{3}$ phase has a three-sublattice structure where twice the setting angles on different sublattices differs by 120° from each other. The system is invariant with respective to the global rotation. In addition, this phase has the symmetry of the direct product of an XY model with an Ising model. This kind of symmetry was noted and investigated previously in the antiferromagnetic XY model ($\alpha>0$ and $\beta=0$ in our notation) by several groups.[12]

Now let us focus on the HB phase. For the HB,c phase, $\langle\cos(2\theta)\rangle$ becomes critical first, so that the setting angle of a rotor is 0° on one sublattice and 90° on the other sublattice. On the other hand, in the HB,s phase, $\langle\sin(2\theta)\rangle$ becomes critical first, so that the setting angle of a rotor is 45° on one sublattice and −45° on the other sublattice. A ground-state calculation as in Eq. (43a) also gives the setting angles as 45° and −45° on the two respective sublattices. It might be possible that the setting angle is 45° near the critical temperature T_c and zero temperature, respectively, and varies with the temperature in between. However, because of the dominance of $\langle\sin(2\theta)\rangle$ over $\langle\cos(2\theta)\rangle$, we find that the setting angle is always 45° over the entire range of temperature below T_c. As described in the Introduction, the experimental observation of the HB setting angle is about 55°.[4] From these results, our conclusion about the model, where we represent the polymer chain with the quadrupole moment only, is that it is not possible to obtain the HB phase with a 55° setting angle. In the following sections, therefore, we will include other interactions to obtain the HB phase with a 55° setting angle.

B. Mean-field theory for the anisotropic model

As we have discussed earlier, one simple way of obtaining a HB phase with a 55° setting angle is to invoke sixfold crystal-field anisotropy. Before we investigate the effects of the anisotropy, we will consider the origin and estimate the magnitude of this type of anisotropy field. Sixfold crystal-field anisotropy of the form of $V_3\cos(6\theta)$ is due to the interaction between a quadrupole moment and mass densities of surrounding rotors. For this kind of interaction the invariant terms are of the following form,

$$v_{ij}=\sum_{k,l} Q_{kl}(\theta_i)x_k(ij)x_l(ij)=a\cos(2\theta_i-2\phi_{ij}) .$$

We assume that the actual interaction between a quadrupole moment and surrounding mass densities can be written in powers of v_{ij} such as

$$V(\theta_i)=V_1'\sum_j v_{ij}+V_2'\sum_j v_{ij}^2+V_3'\sum_j v_{ij}^3+\cdots ,$$

where the summations are not restricted to the nearest neighbors. The first term vanishes and the second term is just a constant due to the sixfold symmetry of the underlying lattice. If we keep only the first nonvanishing term, we have as Eq. (4)

$$V(\theta_i)=V_3\cos(6\theta_i) ,$$

where V_3 is the same order of magnitude as V_3'. Because this interaction is from higher-order terms in powers of v_{ij}, we think that $|V_3|$ will be much smaller compared with other interactions in the problem.

We now investigate the role of lattice anisotropy within the anisotropic model given by

$$H=\alpha\sum_{\langle i,j\rangle}\cos(2\theta_i-2\theta_j)+\beta\sum_{\langle i,j\rangle}\cos(2\theta_i-2\phi_{ij})\cos(2\theta_j-2\phi_{ij})+\sum_j V_3\cos(6\theta_j) , \quad (28)$$

where positive V_3 favors the orientation along the bond direction, and negative V_3 favors the orientation along between the bond directions, in the notation of Fig. 1. To develop mean-field theory we write the single-rotor density matrix as

$$\rho_i(\theta_i)=e^{-h_i(\theta_i)}/(\mathrm{Tr}e^{-h_i(\theta_i)})\equiv e^{-h_i(\theta_i)}/z_i , \quad (29)$$

where

$$h_i(\theta)=(V_3/T)\cos(6\theta)-c\cos(2\theta)-\epsilon_i s\sin(2\theta) , \quad (30)$$

where ϵ_i is $+1$ if i is on one sublattice and -1 if it is on the other sublattice. Thus Eq. (29) provides a definition of the density matrix in terms of order parameters c and s on a two-sublattice structure via the introduction of the parameter ϵ. It is easy to relate averages on one sublattice to those on the other sublattice. Accordingly, we henceforth express our results in terms of only the $\epsilon=1$ sublattice. For instance, using Eq. (29) we find the internal energy per rotor, U, to be

$$U=\tfrac{1}{2}(6\alpha+3\beta)\langle\cos(2\theta)\rangle^2-\tfrac{1}{2}(2\alpha+3\beta)\langle\sin(2\theta)\rangle^2+V_3\langle\cos(6\theta)\rangle , \quad (31)$$

where $\langle f(\theta)\rangle=\mathrm{Tr}[f(\theta)\rho(\theta,\epsilon=1)]$ for any function f. We substitute Eq. (29) into Eq. (10) to find the entropy per rotor as

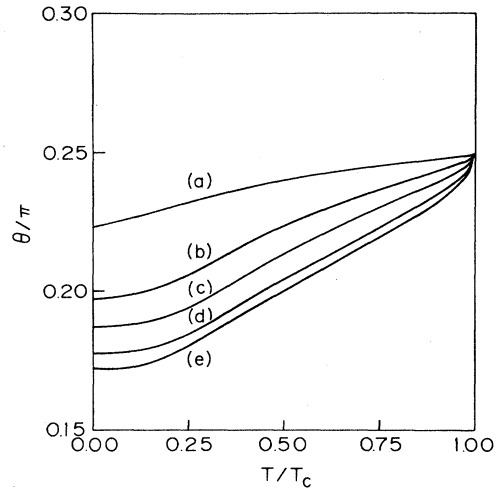

FIG. 4. Setting angle of the HB phase for a model with quadrupole interaction and sixfold crystal-field anisotropy. α and β are chosen to be -1 and 3, respectively, and $T_c=\frac{3}{2}\beta+\alpha=3.5$. Curve (a) is for $V_3=1$, (b) for 2, (c) for 5, (d) for 10, and (e) for 20, in units of $|\alpha|$. The setting angle for the negative values of V_3 can be obtained by reflecting their counterparts for positive V_3 with respect to $y=45°$. Note that for the HB phase with 55° we need a V_3 of about -5.

$$S=(V_3/T)\langle\cos(6\theta)\rangle-c\langle\cos(2\theta)\rangle-s\langle\sin(2\theta)\rangle+\ln z . \quad (32)$$

Observe that we only need to evaluate z to construct the free energy, since

$$\langle\cos(2\theta)\rangle=\partial\ln z/\partial c , \quad (33a)$$

$$\langle\sin(2\theta)\rangle=\partial\ln z/\partial s . \quad (33b)$$

We calculate $\ln z$ to fourth order in the order parameters as

$$\ln z=\ln[2\pi I_0(V_3/T)]+\tfrac{1}{4}(c^2+s^2)-\tfrac{1}{64}(c^2+s^2)^2-\tfrac{1}{24}(c^3-3cs^2)\left[\frac{I_1(V_3/T)}{I_0(V_3/T)}\right] , \quad (34a)$$

where $I_n(x)$ is the modified Bessel function of order n. As we will see, $c\sim s^2$, so that to order s^4 Eq. (34a) is

$$\ln z=\ln[2\pi I_0(V_3/T)]+\tfrac{1}{4}(c^2+s^2)-\tfrac{1}{64}s^4+\tfrac{1}{8}cs^2\left[\frac{I_1(V_3/T)}{I_0(V_3/T)}\right] . \quad (34b)$$

We find the free energy per rotor to fourth order in s as

$$F=\tfrac{1}{2}(6\alpha+3\beta)\left[\tfrac{1}{4}c^2+\tfrac{1}{8}cs^2\left[\frac{I_1(V_3/T)}{I_0(V_3/T)}\right]+\tfrac{1}{64}s^4\left[\frac{I_1(V_3/T)}{I_0(V_3/T)}\right]^2\right]-\tfrac{1}{2}(2\alpha+3\beta)\left[\tfrac{1}{4}s^2-\tfrac{1}{16}s^4+\tfrac{1}{4}cs^2\left[\frac{I_1(V_3/T)}{I_0(V_3/T)}\right]\right]$$
$$+cT\left[\tfrac{1}{2}c+\tfrac{1}{8}s^2\left[\frac{I_1(V_3/T)}{I_0(V_3/T)}\right]\right]+sT\left[\tfrac{1}{2}s-\tfrac{1}{16}s^3+\tfrac{1}{4}cs\left[\frac{I_1(V_3/T)}{I_0(V_3/T)}\right]\right]$$
$$-T\ln[2\pi I_0(V_3/T)]-\tfrac{1}{4}T(c^2+s^2)+\tfrac{1}{64}Ts^4-\tfrac{1}{8}Tcs^2\left[\frac{I_1(V_3/T)}{I_0(V_3/T)}\right], \tag{35}$$

which gives

$$F=\tfrac{1}{4}(T-T_c)s^2+\tfrac{1}{4}[T+\tfrac{1}{2}(6\alpha+3\beta)]c^2+\tfrac{1}{4}cs^2(T+\tfrac{1}{2}\alpha-\tfrac{3}{4}\beta)\left[\frac{I_1(V_3/T)}{I_0(V_3/T)}\right]$$
$$+\tfrac{1}{128}\left[8\alpha+12\beta-6T+(6\alpha+3\beta)\left[\frac{I_1(V_3/T)}{I_0(V_3/T)}\right]^2\right]s^4+F_0(T), \tag{36}$$

where $F_0(T)=-T\ln[2\pi I_0(V_3/T)]$ and $T_c=\frac{1}{2}(2\alpha+3\beta)$. Now we minimize the free energy with respect of c to get the renormalized fourth-order term to be F_4s^4, with

$$F_4=\frac{1}{128}\left[8\alpha+12\beta-6T+(6\alpha+3\beta)\left[\frac{I_1(V_3/T)}{I_0(V_3/T)}\right]^2\right]-\frac{1}{8}\frac{(T+\frac{1}{2}\alpha-\frac{3}{4}\beta)^2}{2T+6\alpha+3\beta}\left[\frac{I_1(V_3/T)}{I_0(V_3/T)}\right]^2. \tag{37}$$

To determine the sign of the fourth-order term at the transition temperature, we set $T=\alpha+3\beta/2$ in Eq. (37),

$$F_4=\tfrac{1}{128}(2\alpha+3\beta)\left[1+\frac{6\alpha+3\beta}{8\alpha+6\beta}\left[\frac{I_1(V_3/T)}{I_0(V_3/T)}\right]^2\right]. \tag{38}$$

Note that the fourth-order term is positive over almost all of the parameter space, which means that a first-order transition does not intervene unless either extreme values of the parameters are admitted, or unless terms of higher than fourth order dominate.

As the temperature is further lowered below transition temperature, the order parameters become larger, and we need next-order terms in the power expansion to describe the critical phenomena with the same accuracy. This is very tedious and inefficient. Therefore, we obtain order parameters c and s self-consistently with numerical iterations as explained before. Self-consistency relations are obtained from Eqs. (15a), (15b), and (31):

$$c=-\frac{2}{T}(3\alpha+\tfrac{3}{2}\beta)\langle\cos(2\theta)\rangle, \tag{39a}$$

$$s=\frac{2}{T}(\alpha+\tfrac{3}{2}\beta)\langle\sin(2\theta)\rangle. \tag{39b}$$

Once we obtain c and s for a given V_3, the density matrix ρ is given as a function of an angle θ by Eq. (29). We then determine the angle $\theta_{\max}$ at which the density matrix becomes maximum. The angle $\theta_{\max}$ is taken as the setting angle of the HB phase and plotted in Fig. 4. Curves (a), (b), (c), (d), and (e) are for $V_3=1$, 2, 5, 10, and 20, respectively, in units of $|\alpha|$. Curves for negative values of V_3 can be obtained by reflecting their counterparts for positive values with respect to $y=45°$ axis. We estimate that V_3 should be roughly -5 to produce an experimentally observed value of about 55°, interpreting this observed angle as the low-temperature value of Fig. 4. As we have discussed before, because the crystal-field anisotropy involves high-order terms in powers of v_{ij}, we think that $|V_3|$ will be much smaller than $5|\alpha|$, which is the approximate magnitude of V_3 needed to produce a 55° HB phase. Therefore, we think that the HB phase with a 55° setting angle is not likely due to the crystal-field anisotropy.

C. Mean-field analyses of the 2-4 model

As we have seen in Sec. III A, the setting angle of HB phase for the 2 model is 45° independent of temperature, whereas the experimental observation is about 55° with respect to the x axis in the notation of Fig. 1. In Sec. III B, we have found that the crystal-field anisotropy would make the angle deviate from 45° and be dependent on the temperature. The angle increases for negative V_3 and decreases for positive V_3. However, as discussed in Sec. III B, an unphysically large value of V_3 of around $-5|\alpha|$ is needed to explain the experimentally observed setting angle of about 55°. Therefore, we consider other interactions such as dipole and octopole, which have a different angular dependence from the quadrupole interaction. The motivation is that below some critical temperature any order parameter of the competing interactions is not vanishing, and the competition between these interactions of different angular dependence may produce HB phase with the setting angle of about 55°. We will first consider a model with quadrupole and octopole interaction, referred to as the 2-4 model, in Sec. III C, and a model with quadrupole and dipole interactions, the 2-1 model, in Sec. III D.

The orientation energy for the 2-4 model is given by Eq. (5),

$$H=\alpha\sum_{\langle i,j\rangle}\cos(2\theta_i-2\theta_j)+\beta\sum_{\langle i,j\rangle}\cos(2\theta_i-2\phi_{ij})\cos(2\theta_j-2\phi_{ij})+\lambda\alpha\sum_{\langle i,j\rangle}\cos(4\theta_i-4\theta_j)$$
$$+\lambda\beta\sum_{\langle i,j\rangle}\cos(4\theta_i-4\phi_{ij})\cos(4\theta_j-4\phi_{ij})\ , \tag{5'}$$

where λ is the ratio of octopole to quadrupole interactions. Because we are interested in modeling the interchain ordering of pristine $(CH)_x$, which was observed to have HB structure, we choose $\alpha=-1$ and $\beta>\frac{4}{3}$. α is chosen negative to be consistent with electrostatic interaction. In most cases, β will be chosen to be within the range of 2–4.

Mean-field analyses for the 2-4 model can be formulated by taking the single-rotor density matrix as

$$\rho_i(\theta_i)=\frac{1}{Z_i}\exp[C_2\cos(2\theta_i)+S_2\sin(2\theta_i)+C_4\cos(4\theta_i)+S_4\sin(4\theta_i)]\ , \tag{40}$$

where

$$Z_i=\mathrm{Tr}\{\exp[C_2\cos(2\theta_i)+S_2\sin(2\theta_i)+C_4\cos(4\theta_i)+S_4\sin(4\theta_i)]\}\ ,$$

where S_2 and S_4 should be replaced by $-S_2$ and $-S_4$, respectively, on the other sublattice. Thus Eq. (40) provides a definition of the density matrix in terms of order parameters C_2, S_2, C_4, and S_4. The internal energy per rotor is given by

$$U=\frac{1}{N}\sum_{\langle i,j\rangle}\Bigg[\left[\alpha+\frac{\beta}{2}[1+\cos(4\phi_{ij})]\right]\langle\cos(2\theta_i)\rangle\langle\cos(2\theta_j)\rangle+\left[\alpha+\frac{\beta}{2}[1-\cos(4\phi_{ij})]\right]\langle\sin(2\theta_i)\rangle\langle\sin(2\theta_j)\rangle$$
$$+\frac{\beta}{2}\sin(4\phi_{ij})[\langle\sin(2\theta_i)\rangle\langle\cos(2\theta_j)\rangle+\langle\cos(2\theta_i)\rangle\langle\sin(2\theta_j)\rangle]$$
$$+\lambda\left[\alpha+\frac{\beta}{2}[1+\cos(8\phi_{ij})]\right]\langle\cos(4\theta_i)\rangle\langle\cos(4\theta_j)\rangle+\lambda\left[\alpha+\frac{\beta}{2}[1-\cos(8\phi_{ij})]\right]\langle\sin(4\theta_i)\rangle\langle\sin(4\theta_j)\rangle$$
$$+\lambda\frac{\beta}{2}\sin(8\phi_{ij})[\langle\sin(4\theta_i)\rangle\langle\cos(4\theta_j)\rangle+\langle\cos(4\theta_i)\rangle\langle\sin(4\theta_j)\rangle]\Bigg] \tag{41a}$$
$$=(3\alpha+\tfrac{3}{2}\beta)\langle\cos(2\theta)\rangle^2-(\alpha+\tfrac{3}{2}\beta)\langle\sin(2\theta)\rangle^2+\lambda(3\alpha+\tfrac{3}{2}\beta)\langle\cos(4\theta)\rangle^2-\lambda(\alpha+\tfrac{3}{2}\beta)\langle\sin(4\theta)\rangle^2\ . \tag{41b}$$

Self-consistency relations are obtained from Eqs. (15a), (15b), and (41b) as follows:

$$C_2=-\frac{2}{T}(3\alpha+\tfrac{3}{2}\beta)\langle\cos(2\theta)\rangle\ , \tag{42a}$$

$$S_2=\frac{2}{T}(\alpha+\tfrac{3}{2}\beta)\langle\sin(2\theta)\rangle\ , \tag{42b}$$

$$C_4=-\frac{2}{T}\lambda(3\alpha+\tfrac{3}{2}\beta)\langle\cos(4\theta)\rangle\ , \tag{42c}$$

$$S_4=\frac{2}{T}\lambda(\alpha+\tfrac{3}{2}\beta)\langle\sin(4\theta)\rangle\ . \tag{42d}$$

We take arbitrary initial configurations for C_2, S_2, C_4, and S_4 and solve Eqs. (42) until the self-consistency is satisfied. Without consideration of terms in the free energy higher than the second-order ones, there is criticality of $\langle\sin(2\theta)\rangle$ at $T_{c,2}=\alpha+\frac{3}{2}\beta$ and of $\langle\sin(4\theta)\rangle$ at $T_{c,4}=\lambda T_{c,2}$. Higher-order terms renormalize the lower of the two critical temperatures; that is, for $\lambda<\lambda_c=1$ $T_{c,4}$ is renormalized and for $\lambda>\lambda_c$ $T_{c,2}$ is renormalized. Note that at $\lambda=1$ the transition lines for 2θ and 4θ ordering cross. Detailed Landau expansion near this tetracritical point of $\lambda=\lambda_c=1$ is presented in Appendix A. The phase diagram in the T-λ plane obtained in the mean-field analyses described above is shown in Fig. 5. There are four phases, labeled DS, I, II, and III, separated by critical temperatures $T_{c,2}(\lambda)$ and $T_{c,4}(\lambda)$. Note the renormalization of critical temperatures. DS represents disordered phase where all four of the order parameters C_2, S_2, C_4, and S_4 vanish. In phase I, S_2 and C_4 are nonvanishing, and in phase II, only S_4 is nonvanishing. In phase III, none of the four order parameters is vanishing. Because there are three possible orientations for the HB phase related by $\pm2\pi/3$ rotation from the other orientations, there is a possibility that the direction of the HB phase associated with quadrupole interactions can be different from that associated with octopole ones. This situation is possible only in phase III, because none of the order parameters describing quadrupole ordering (C_2 and S_2) and octopole ordering (C_4 and S_4) is vanishing in phase III. It is easy to see by superposing two HB phases with different orientations that a unit cell is composed of four sublattices. Therefore, the situation where the direction of the HB phase associated with quadrupole interaction is different from that with the octopole one is realized by a four-sublattice structure instead of a two-

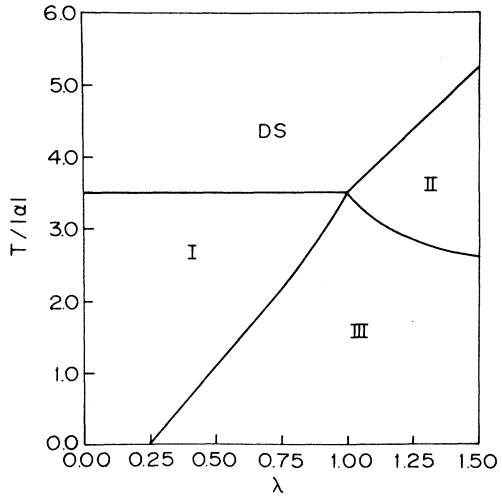

FIG. 5. Phase diagram of the 2-4 model in the T-λ plane with $\alpha=-1$ and $\beta=3$. DS represents disordered phases where all order parameters vanish. In phase I the order parameters S_2 and C_4 are nonvanishing, in phase II only S_4 is nonvanishing, and in phase III all four order parameters are nonvanishing. The setting angle is 45° in phase I, 22.5° (67.5°) in phase II, and it varies with temperature and λ in phase III. There are two degenerate states of the setting angle related by a reflection with respect to the $y=45°$ axis in phases II and III.

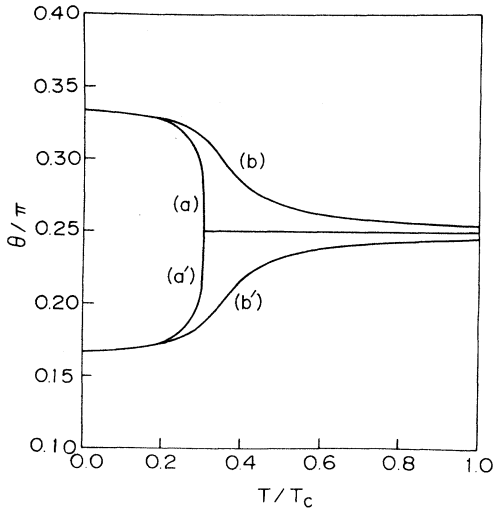

FIG. 6. Setting angle of the HB phase as a function of temperature at a fixed λ. This plot corresponds to a cut parallel to the y axis of Fig. 5 at $\lambda=0.5$, scanning through phases I and III. Curves (a) and (a') are two degenerate branches of the setting angle for $V_3=0$. For nonzero V_3, this degeneracy is lifted, curve (b) is for $V_3=-0.1$, and (b') is for $V_3=0.1$.

sublattice one. The latter one is realized when the same orientation is favored. As shown in Eqs. (A14) and (A15) of Appendix A with a Landau expansion, the same orientation is favored if $4\alpha+\beta<0$ and a different one is favored otherwise. We also confirmed this result with self-consistent mean-field calculations by taking a four-site unit cell. We therefore take $\beta<4$ in this study to ensure that the two-sublattice HB phase is realized.

Once we obtain the order parameters C_2, S_2, C_4, and S_4, then the density matrix ρ is specified as a function of an angle θ. We then find $\theta_{\max}$ at which ρ becomes maximum and take $\theta_{\max}$ as the setting angle of the HB structure. One interesting observation about the 2-4 model is that there are two degenerate states[13] of solutions $\theta_{\max}(T)$ and $\theta'_{\max}(T)$ related by $\theta_{\max}(T)=\pi/2-\theta'_{\max}(T)$. In other words, one branch of the setting angle is obtained by a reflection of the other branch about the $y=45°$ axis. This degeneracy can easily be seen by substituting $\pi/2-\theta$ for θ in the free energy of the 2-4 model given by Eq. (13) with Eq. (41b). Under the operation of $\theta\rightarrow\pi/2-\theta$, we have $\cos(2\theta)\rightarrow-\cos(2\theta)$, $\sin(2\theta)\rightarrow\sin(2\theta)$, $\cos(4\theta)\rightarrow\cos(4\theta)$, and $\sin(4\theta)\rightarrow-\sin(4\theta)$, and the internal energy is even (quadratic) function of $\langle\cos\rangle$'s and $\langle\sin\rangle$'s. Therefore, the free energy is invariant under the operation of $C_2\rightarrow-C_2$, $S_2\rightarrow S_2$, $C_4\rightarrow C_4$, and $S_4\rightarrow-S_4$. This twofold degeneracy also can easily be demonstrated by calculating the internal energy, as we will see later. For $\lambda<\lambda_c^{(0)}=\frac{1}{4}$ the setting angle is 45°, independent of temperature. For $\lambda_c^{(0)}<\lambda<\lambda_c=1$, however, the angle is 45° between $T_{c,2}$ and $T_{c,4}(\lambda)$, and below $T_{c,4}(\lambda)$ the angle is not 45° any more and can be either greater or smaller than 45° due to the twofold degeneracy, as was discussed. If $\lambda>\lambda_c$, $\langle\sin(4\theta)\rangle$ becomes critical first as temperature is reduced. Hence, the setting angle is 22.5° (65.5°) between $T_{c,4}$ and $T_{c,2}(\lambda)$ and increases (decreases) as temperature is lowered below $T_{c,2}(\lambda)$. The preceding arguments are shown in Fig. 6 for a representative value of λ, for example, $\lambda=0.5$. Curves (a) and (a') are the two branches of the setting angle of the HB phase as a function of temperature for $\beta=3$. Note that the setting angle is 45° independent of temperature between $T_{c,2}$ and $T_{c,4}(\lambda)$.

The existence of $\lambda_c^{(0)}$ at zero temperature and the asymptotic behavior of setting angles can be checked against the ground-state calculations at zero temperature. The energy on a two-sublattice structure as a function of angles θ,θ' is calculated by use of Eq. (5'),

$$E(\theta,\theta')=E_2(\theta,\theta')+E_4(\theta,\theta') ,$$

where

$$E_2(s,\Delta)=\alpha[1+2\cos(2\Delta)]+\frac{\beta}{2}[1+\cos(2s)\cos(2\Delta)+2\cos(2\Delta)-\cos(2s)] , \tag{43a}$$

$$E_4(s,\Delta)=\lambda\alpha[1+2\cos(4\Delta)]+\lambda\frac{\beta}{2}[1+\cos(4s)\cos(4\Delta)+2\cos(4\Delta)-\cos(4s)] , \tag{43b}$$

where $s\equiv\theta+\theta'$ and $\Delta\equiv\theta-\theta'$. Minimizing $E(s,\Delta)$ with respect to s gives $s=0$ for $\beta>0$. Therefore, $\theta'=-\theta$, in agree-

ment with HB structure. Then $E(s,\Delta)$ is reduced to

$$E(\Delta)=\alpha[1+2\cos(2\Delta)]+\tfrac{3}{2}\beta\cos(2\Delta)+\lambda\alpha[1+2\cos(4\Delta)]+\lambda\tfrac{3}{2}\beta\cos(4\Delta)\ . \tag{44a}$$

Note that the internal energy given by Eq. (44a) is invariant under the operation of $\Delta\rightarrow\pi-\Delta$. We rewrite this apart from constant terms with $\cos(2\Delta)\equiv t$ as

$$E(t)=(2\alpha+\tfrac{3}{2}\beta)[t+\lambda(2t^2-1)]\ , \tag{44b}$$

which for $\lambda>0$ is minimized when

$$t=\cos(2\Delta)=-\frac{1}{4\lambda}\ . \tag{45}$$

The angles Δ calculated numerically agree extremely well with Eq. (45).

Effects of crystal-field anisotropy of the form given by Eq. (4) can be studied by extending the single-rotor density matrix as follows:

$$\rho_i(\theta_i)=\frac{1}{Z_i}\exp\left[C_2\cos(2\theta_i)+S_2\sin(2\theta_i)+C_4\cos(4\theta_i)+S_4\sin(4\theta_i)-\frac{V_3}{T}\cos(6\theta_i)\right]\ , \tag{46}$$

where

$$Z_i=\mathrm{Tr}\left\{\exp[C_2\cos(2\theta_i)+S_2\sin(2\theta_i)+C_4\cos(4\theta_i)+S_4\sin(4\theta_i)-\frac{V_3}{T}\cos(6\theta_i)]\right\}\ .$$

$V_3\langle\cos(6\theta)\rangle$ should be added to the internal energy, but because this extra term is linear in the order parameter it is canceled exactly by the contribution from entropy. The self-consistency relations of Eq. (42) remain the same, even though the values of the order parameters are changed. We iterate the same procedures as before, including sixfold crystal-field anisotropy, and find that the anisotropy field destroys the critical behavior associated with the lower critical temperature and resolves the twofold degeneracy of the setting angle. In Fig. 6, we plot the setting angle of the HB phase as a function of temperature for $\lambda=0.5$. Curves (a) and (a′) are two branches of the solution for $V_3=0$. Nonzero V_3 resolves this degeneracy, as can be seen by substituting $\theta\rightarrow\pi/2-\theta$ in Eq. (46); for $V_3>0$, the branch with the smaller angle is favored and for $V_3<0$ that with the larger one is favored. Curve (b) is for $V_3=0.1$, and curve (b′) is for $V_3=-0.1$. The absence of the critical behavior associated with the lower transition temperature can clearly be seen for nonzero V_3.

D. Mean-field analyses of the 2-1 model

In the previous subsection we showed that the competition between interactions of different angular dependence results in a HB phase with a setting angle different from 45°. Although this 2-4 model can produce a HB phase with a 55° setting angle, there are some problems which prevent us from directly interpreting the interchain orientational ordering phenomena in terms of this model. First, there is a twofold degeneracy in the setting angle of the HB phase. This implies that a 35° setting angle should be observed as well as a 55° one. Crystal-field anisotropy will resolve this degeneracy, but because of the smallness of V_3 both branches of the setting angle should still be observable. Second, the fact that the polymer chain is not symmetric under the rotation by π about an axis parallel to the chain direction implies that the polymer chain ought to be represented by a rotor with nonvanishing dipolar interaction. In this section, therefore, we will include the dipole interaction in addition to the quadrupole one. As we will see later, this dipole term resolves the twofold degeneracy.

The 2-1 model, which includes quadrupole and dipole interactions, can be analyzed in the exact same way as the 2-4 model. The orientational energy for the 2-1 model is given by

$$H=\alpha\sum_{\langle i,j\rangle}\cos(2\theta_i-2\theta_j)+\beta\sum_{\langle i,j\rangle}\cos(2\theta_i-2\phi_{ij})\cos(2\theta_j-2\phi_{ij})-\lambda\alpha\sum_{\langle i,j\rangle}\cos(\theta_i-\theta_j)-\lambda\beta\sum_{\langle i,j\rangle}\cos(\theta_i-\phi_{ij})\cos(\theta_j-\phi_{ij})\ , \tag{6′}$$

where λ is the ratio of dipole to quadrupole interactions. Note that we have a minus sign in front of λ. A simpler version of the 2-1 model ($\alpha<0$ and $\beta=0$) has been studied by Lee *et al.*[14] It was shown that this simple model has very interesting phenomena, such as half-vortices and "string"-excitations in addition to the usual integer vortices. It remains to be seen to what extent the anisotropic part of interaction [nonzero β in Eq. (6′)] will change the dynamics of the mod-

el. The single-rotor density matrix is taken in the same way as for the 2-4 model,

$$\rho_i(\theta_i)=\frac{1}{Z_i}\exp[C_2\cos(2\theta_i)+S_2\sin(2\theta_i)+C_1\cos(\theta_i)+S_1\sin(\theta_i)] , \tag{47}$$

where

$$Z_i=\mathrm{Tr}\{\exp[C_2\cos(2\theta_i)+S_2\sin(2\theta_i)+C_1\cos(\theta_i)+S_1\sin(\theta_i)]\} .$$

Contribution to the internal energy from dipole interactions is calculated assuming the two-sublattice structure shown in Fig. 1 as follows:

$$U_1=-\frac{\lambda}{N}\sum_{\langle i,j\rangle}\left[\left[\alpha+\frac{\beta}{2}[1+\cos(2\phi_{ij})]\right]\langle\cos(\theta_i)\rangle\langle\cos(\theta_j)\rangle+\left[\alpha+\frac{\beta}{2}[1-\cos(2\phi_{ij})]\right]\langle\sin(\theta_i)\rangle\langle\sin(\theta_j)\rangle\right] . \tag{48a}$$

Terms involving $\sin(2\phi_{ij})$ vanish for the two-sublattice structure, and the summations in Eq. (48a) are carried out to yield

$$U_1=-\lambda\left[\tfrac{1}{2}\alpha[\langle\cos(\theta)\rangle\langle\cos(\theta)\rangle+\langle\cos(\theta)\rangle'\langle\cos(\theta)\rangle']+2(\alpha+\tfrac{3}{4}\beta)\langle\cos(\theta)\rangle\langle\cos(\theta)\rangle'\right.$$
$$\left.+\tfrac{1}{2}(\alpha+\beta)[\langle\sin(\theta)\rangle\langle\sin(\theta)\rangle+\langle\sin(\theta)\rangle'\langle\sin(\theta)\rangle']+2\left[\alpha+\frac{\beta}{4}\right]\langle\sin(\theta)\rangle\langle\sin(\theta)\rangle'\right] , \tag{48b}$$

where $\langle\cos(\theta)\rangle$ represents the thermal average of $\cos(\theta)$ on one sublattice and $\langle\cos(\theta)\rangle'$ on the other sublattice. To be consistent with the symmetry determined experimentally, we require

$$\langle\cos(\theta)\rangle'=\langle\cos(\theta)\rangle$$

and

$$\langle\sin(\theta)\rangle'=-\langle\sin(\theta)\rangle .$$

Then Eq. (48b) is reduced to

$$U_1=-\lambda(3\alpha+\tfrac{3}{2}\beta)\langle\cos(\theta)\rangle^2-\lambda\left[\frac{\beta}{2}-\alpha\right]\langle\sin(\theta)\rangle^2 . \tag{48c}$$

Note that U_1 is not invariant under the operation of $\theta\rightarrow\pi/2-\theta$. Other requirements to be consistent with HB symmetry are that $\langle\sin(\theta)\rangle$ should become critical first as temperature is lowered and $\lambda(\beta/2-\alpha)$ should be positive. These are satisfied by taking $\beta<4$ and $\lambda>0$. In fact, $\beta>\frac{2}{5}$ should also be satisfied to have a HB phase, as shown in Fig. 2(a). Internal energy is then obtained from Eqs. (41b) and (48c),

$$U=(3\alpha+\tfrac{3}{2}\beta)\langle\cos(2\theta)\rangle^2-(\alpha+\tfrac{3}{2}\beta)\langle\sin(2\theta)\rangle^2$$
$$-\lambda(3\alpha+\tfrac{3}{2}\beta)\langle\cos(\theta)\rangle^2-\lambda(\tfrac{1}{2}\beta-\alpha)\langle\sin(\theta)\rangle^2 \tag{49}$$

and the self-consistency relations are

$$C_2=-\frac{2}{T}(3\alpha+\tfrac{3}{2}\beta)\langle\cos(2\theta)\rangle , \tag{50a}$$

$$S_2=\frac{2}{T}(\alpha+\tfrac{3}{2}\beta)\langle\sin(2\theta)\rangle , \tag{50b}$$

$$C_1=\frac{2}{T}\lambda(3\alpha+\tfrac{3}{2}\beta)\langle\cos(\theta)\rangle , \tag{50c}$$

$$S_1=\frac{2}{T}\lambda(\tfrac{1}{2}\beta-\alpha)\langle\sin(\theta)\rangle . \tag{50d}$$

Numerical procedures are the same as described before.

As is the case with the 2-4 model, there is a critical value λ_c at which the crossover between critical behaviors associated with $\langle\sin(2\theta)\rangle$ and $\langle\sin(\theta)\rangle$ occurs. For the 2-1 model, however, λ_c depends on β. We find

$$\lambda_c=(\tfrac{3}{2}\beta-1)/(\tfrac{1}{2}\beta+1) . \tag{51}$$

Zero-temperature calculations are also carried out. The energy on a two-sublattice structure as a function of angles θ,θ' is given by

$$E(s,\Delta)=E_2(s,\Delta)+E_1(s,\Delta) ,$$

where $s\equiv\theta+\theta'$ and $\Delta\equiv\theta-\theta'$. $E_2(s,\Delta)$ is given by Eq. (43a) and

$$E_1(s,\Delta)=-\lambda\alpha[1+2\cos(\Delta)]$$
$$-\lambda\frac{\beta}{2}[2\cos(\Delta)+\cos(s)+1-\cos(s)\cos(\Delta)] . \tag{52}$$

Setting $s=0$, $E(s,\Delta)$ is reduced apart from a constant to

$$E(\Delta)=(\tfrac{3}{2}\beta+2\alpha)[2\cos^2(\Delta)-1]-\lambda(2\alpha+\tfrac{1}{2}\beta)\cos(\Delta) , \tag{53}$$

which is minimized at

$$\cos(\Delta)=\frac{\lambda}{4}\frac{\frac{1}{2}\beta+2\alpha}{\frac{3}{2}\beta+2\alpha}=\frac{\lambda}{4}\frac{\frac{1}{2}\beta-2}{\frac{3}{2}\beta-2} . \tag{54}$$

$\lambda_c^{(0)}$ is determined from $\cos(\Delta)=-1$ to be

$$\lambda_c^{(0)}=(8-6\beta)/(\tfrac{1}{2}\beta-2) . \tag{55}$$

Order parameters C_2, S_2, C_1, and S_1 are determined self-consistently. We then have the density matrix ρ as a function of an angle θ, and find $\theta_{\max}$ at which ρ becomes maximum. $\theta_{\max}$ is taken as the setting angle of the HB

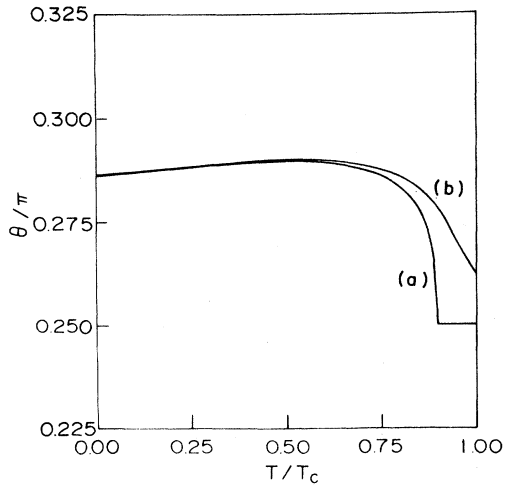

FIG. 7. Setting angle of the HB phase of the 2-1 model as a function of temperature at $\lambda=0.9$ and $\beta=2$. Curve (a) is for $V_3=0$ and (b) is for $V_3=0.1$. Note that there is no degeneracy in the 2-1 model.

phase. In Fig. 7 we plot the setting angle as a function of temperature for $\lambda=0.9$ and $\beta=2$, where $\lambda_c=1$ as given by Eq. (51). Curve (a) is for $V_3=0$ and (b) is for $V_3=0.1$. Note that the critical behavior associated with the lower transition temperature is removed for nonzero V_3, as is the case with the 2-4 model. Equation (54), which gives twice the setting angles at zero temperature as a function of λ and β, can be used to guide us in taking appropriate values of λ and β, which will produce a 55° HB phase. λ is restricted by Eq. (51), which gives the upper limit if we want a 45° HB phase near $T_{c,2}$. Of course, without available experimental data to compare with, we cannot make strong arguments at this point.

IV. SPIN-WAVE SPECTRUM OF ROTORS

In Sec. III, we studied several models, such as the 2, 2-4, and 2-1 models, and found that various ordered phases, such as the temperature and the interaction parameters, are varied, without considering the low-lying excitations. As is well known, long-wavelength soft-mode fluctuations of phonons or spin waves destroy conventional long-range order in two dimensions. Therefore, we will focus our attention on the spin-wave excitations in the problem and investigate the stability of the HB phase. The gapless spectrum of a spin implies a Mermin-Wagner instability in two dimensions, but nonvanishing gap guarantees the stability of the HB phase. We will present our analyses for the 2-4 model. Analyses for other models can be carried out in the same way. Now let us study the spin-wave spectrum and stability of the herringbone 45° (HB-45) phase of the 2-4 model. However, because we will want to consider spin waves in the general herringbone phase (GHB), where the angles of the molecules with respect to the modulation vector of the phase are not restricted to be 45°, we will keep this angle unspecified in our formulation.

We treat the GHB phase in which there are two sublattices labeled by a and b. The molecules are at sites $\mathbf{R}$ and $\mathbf{R}+\frac{1}{2}\mathbf{b}_2$, where the lattice basis vectors are

$$\mathbf{b}_1=a\hat{\mathbf{j}},\quad \mathbf{b}_2=a(\sqrt{3}\hat{\mathbf{i}}+\hat{\mathbf{j}}), \tag{56}$$

and the reciprocal-lattice basis vectors are

$$\mathbf{G}_1=\frac{2\pi}{\sqrt{3}a}(-\hat{\mathbf{i}}+\sqrt{3}\hat{\mathbf{j}}),\quad \mathbf{G}_2=\frac{2\pi}{\sqrt{3}a}\hat{\mathbf{i}}. \tag{57}$$

Note that $\mathbf{G}_1+\mathbf{G}_2=(2\pi/a)\hat{\mathbf{j}}$. We find that the first Brillouin zone is defined by

$$|q_x|<\pi/(\sqrt{3}a),\quad |q_y|<\pi/a. \tag{58}$$

The potential energy per rotor is thus

$$V=\sum_{\mathbf{R}}\tfrac{1}{2}[H(a,\mathbf{R};b,\mathbf{R}-\mathbf{b}_2)+H(a,\mathbf{R};b,\mathbf{R}+\mathbf{b}_1-\mathbf{b}_2)+H(a,\mathbf{R};a,\mathbf{R}+\mathbf{b}_1)$$
$$+H(a,\mathbf{R};b,\mathbf{R})+H(a,\mathbf{R};b,\mathbf{R}-\mathbf{b}_1)+H(b,\mathbf{R};b,\mathbf{R}+\mathbf{b}_1)], \tag{59}$$

where $a,\mathbf{R}$ labels a rotor at position $\mathbf{r}(a,\mathbf{R})\equiv\mathbf{R}$ and the label $b,\mathbf{R}$ refers to the one at position $\mathbf{r}(b,\mathbf{R})\equiv\mathbf{R}+\frac{1}{2}\mathbf{b}_2$, and H is given by Eq. (5) with Eqs. (1) and (3). Explicit expressions for each term of Eq. (59) is given in Appendix C. We set

$$\theta_{a,\mathbf{R}}=\theta_0+u_{a,\mathbf{R}},\quad \theta_{b,\mathbf{R}}=-\theta_0+u_{b,\mathbf{R}}. \tag{60}$$

Up to linear order in the u's we have

$$V=V_0+V_1\sum_{\mathbf{R}}(u_{b,\mathbf{R}}-u_{a,\mathbf{R}}), \tag{61}$$

where

$$V_1=\sin(4\theta_0)[(4\alpha+3\beta)+4(4\alpha_4+3\beta_4)\cos(4\theta_0)] \tag{62a}$$
$$=\sin(4\theta_0)(4\alpha+3\beta)[1+4\lambda\cos(4\theta_0)]. \tag{62b}$$

Equilibrium requires $V_1=0$. Thus we have

$$\theta_0=\tfrac{1}{4}\pi,\quad |\lambda|<\tfrac{1}{4} \tag{63a}$$
$$\cos(4\theta_0)=-1/4\lambda,\quad |\lambda|>\tfrac{1}{4}. \tag{63b}$$

Since we are only interested in relatively small values of λ, we do not explore the upper limit in $|\lambda|$ for which Eq. (63b) holds. Note the degeneracy between the two solutions of Eq. (63b) for θ_0: one solution has $\theta_0<\pi/4$; the other has $\theta_0>\pi/4$.

Neglecting the constant V_0, we expand V up to quadratic order in the u's, and then take the Fourier transform as

$$u_{a,\mathbf{R}}=\frac{1}{\sqrt{N}}\sum_{\mathbf{q}}u_a(\mathbf{q})e^{i\mathbf{q}\cdot\mathbf{R}},\quad u_{b,\mathbf{R}}=\frac{1}{\sqrt{N}}\sum_{\mathbf{q}}u_b(\mathbf{q})e^{i\mathbf{q}\cdot\mathbf{R}}. \tag{64}$$

Then we obtain

$$V=\frac{1}{2}\sum_{\mathbf{q}}[D_{a,a}(\mathbf{q})u_a(\mathbf{q})u_a(-\mathbf{q})+D_{a,b}(\mathbf{q})u_a(\mathbf{q})u_b(-\mathbf{q})+D_{b,a}(\mathbf{q})u_b(\mathbf{q})u_a(-\mathbf{q})+D_{b,b}(\mathbf{q})u_b(\mathbf{q})u_b(-\mathbf{q})] , \tag{65}$$

where

$$D_{a,a}(\mathbf{q})=-\alpha[8\cos(4\theta_0)+4]-\alpha_4(32\cos(8\theta_0)+16]+\beta[6-12\cos^2(2\theta_0)]+\beta_4(24-48\cos^2(4\theta_0)]$$
$$+[4\alpha+16\alpha_4+4\beta\sin^2(2\theta_0)+16\beta_4\sin^2(4\theta_0)]\cos(\mathbf{q}\cdot\mathbf{b}_1) , \tag{66a}$$

$$D_{a,b}(\mathbf{q})=\{2\alpha\cos(4\theta_0)+8\alpha_4\cos(62\theta_0)+\tfrac{1}{2}\beta[3-4\sin^2(2\theta_0)]+2\beta_4[3-4\sin^2(4\theta_0)]\}(1+e^{i\mathbf{q}\cdot\mathbf{b}_2}+e^{i\mathbf{q}\cdot(\mathbf{b}_2-\mathbf{b}_1)}+e^{i\mathbf{q}\cdot\mathbf{b}_1}) , \tag{66b}$$

$$D_{b,a}(\mathbf{q})=D_{a,b}(-\mathbf{q}) , \tag{66c}$$

$$D_{b,b}(\mathbf{q})=D_{a,a}(\mathbf{q}) . \tag{66d}$$

The eigenvalues of D are

$$\omega_{\pm}=D_{a,a}(\mathbf{q})\pm|D_{a,b}(\mathbf{q})| . \tag{67}$$

Note that there is a degeneracy between θ_0 and $\pi/2-\theta_0$ for $\omega_{\pm}$, in agreement with the previous analysis in Sec. III C.

We now refer to the HB-45 phase, by setting $\theta_0=\pi/4$. Then, we obtain the eigenvalues of D as

$$\omega_{\pm}=4\alpha-48\alpha_4+6\beta-24\beta_4+(4\alpha+4\beta+16\alpha_4)\cos(\mathbf{q}\cdot\mathbf{b}_1)\pm(-2\alpha+8\alpha_4-\tfrac{1}{2}\beta+6\beta_4)|1+e^{i\mathbf{q}\cdot\mathbf{b}_1}|\,|1+e^{i\mathbf{q}\cdot(\mathbf{b}_2-\mathbf{b}_1)}| . \tag{68}$$

We can check this by comparing with the energy of the two-sublattice structure when one sublattice has an angle θ and the other θ' given by Eqs. (43). We set $s=x$ and $\Delta=\pi+y$ in Eq. (43) and expand for small x and y. Then, we find two modes:

$$V=(4\beta)x^2 , \tag{69a}$$

$$V=(6\beta+8\alpha-24\beta_4-32\alpha_4)y^2 , \tag{69b}$$

which give the zero-wave-vector eigenvalues:

$$\omega_+=8\beta,\quad \omega_-=12\beta+16\alpha-48\beta_4-64\alpha_4 , \tag{70}$$

which agrees with Eq. (68) for $\mathbf{q}=\mathbf{0}$.

Now we wish to analyze the stability of the spin-wave spectrum of the HB-45 phase. So we wish to find out the conditions under which one of the $\omega_{\pm}$ can become negative. As λ [of Eq. (3)] is increased, one sees that one of the $\omega_{\pm}$ will become negative when $D_{\alpha,\beta}$ is maximal for a fixed value of α,β. This reasoning indicates that we should investigate the case $q_x=0$. Thus we set $\mathbf{q}=q\hat{\mathbf{j}}$ and we have

$$\omega_{\pm}=8\alpha-96\alpha_4+12\beta-48\beta_4+(8\alpha+8\beta+32\alpha_4)\cos(aq)$$
$$\pm(-8\alpha-2\beta+32\alpha_4+24\beta_4)|1+e^{iaq}| . \tag{71}$$

We now set $\cos(qa)=2\cos^2(qa/2)-1$ and $|1+e^{iaq}|=2\cos(qa/2)$, so that

$$\omega_{\pm}=4\beta-128\alpha_4-48\beta_4\pm(-16\alpha-4\beta+64\alpha_4+48\beta_4)z$$
$$+(16\alpha+16\beta+64\alpha_4)z^2 , \tag{72}$$

where $z=\cos(qa/2)$, which is $0\le z\le 1$ within the first Brillouin zone. Alternatively, we may consider only ω_+, but allow z to range over the entire interval $|z|<1$. Then we interpret negative z in ω_+ as being equivalent to $-z$ in ω_-.

To investigate the minimum values of ω_+, we set $z=\pm1$ or extremize ω_+. The actual minimum is the smallest of these three candidates. The first two candidates are

$$\omega_+(z=1)=8\beta , \tag{73a}$$

$$\omega_+(z=-1)=12\beta+16\alpha-64\alpha_4-48\beta_4=\omega_-(z=1) . \tag{73b}$$

We find that for $\beta<\beta_c=\frac{21}{8}$, the eigenvalue which first becomes negative is

$$\omega_-(\mathbf{q}=\mathbf{0})=(16\alpha+12\beta)(1-4\alpha)$$
$$=(64\alpha+48\beta)(\lambda_c-\lambda) . \tag{74}$$

However, for $\beta>\beta_c$ and $16\lambda+12\beta\lambda-9\beta<-\frac{47}{4}$, the mode which becomes soft first occurs at a wave vector different from the zone center, which implies an instability at a longitudinally modulated phase. This needs further study. The transition between the HB-45 and GHB phases at $\lambda=\lambda_c=\frac{1}{4}$ is signaled by the fact that the energy gap $(\omega_-)^{1/2}$ at the zone center vanishes as $\lambda\to\lambda_c$. We can follow the energy gap in the GHB phase for $\lambda>\frac{1}{4}$, where the orientations of the rotors are determined by Eq. (63b). Using Eqs. (66) and (67) then gives

$$\omega_-(\mathbf{q}=\mathbf{0})=(4\alpha+3\beta)(16\lambda^2-1)/\lambda$$
$$\sim(128\alpha+96\beta)(\lambda-\lambda_c) . \tag{75}$$

Thus we see that the energy gap is vanishing as the phase boundary is approached from within the GHB phase, but with a slope different from that of Eq. (74) within the HB-45 phase. The fact that we have a soft mode at the HB-45→GHB phase boundary means that for a strictly two-dimensional model there is a Mermin-Wagner instability on this phase boundary. It remains to be seen whether or not this phase boundary gives rise to a Kosterlitz-Thouless transition.

V. SUMMARY AND CONCLUDING REMARKS

We have presented our mean-field analysis of various models for the interchain orientational ordering of undoped $(CH)_x$, which we referred to as the 2, 2-4, and 2-1 models, including sixfold crystal-field anisotropy. The polymer chain was modeled by a rotor on a two-dimensional triangular lattice with a combination of quadrupole, dipole, and octopole moments. The relative strengths of these moments can be estimated by comparing with the observed setting angle of the HB phase. The 2 model, which includes the quadrupole interaction only, has been shown to have various phases such as ferromagnetic, $\sqrt{3}\times\sqrt{3}$, HB,*s*, HB,*c*, and longitudinally modulated incommensurate phases as the temperature and interaction parameters are varied. We also have considered the sixfold crystal-field anisotropy due to the interaction between a rotor and surrounding mass densities. Because this is a higher-order contribution, we have concluded that the energy scale associated with the anisotropy should be small compared with those of other interaction terms. For the 2-4 model with parameters chosen in favor of the HB phase, we have shown a phase diagram in the T-λ plane with four phases, labeled DS, I, II, and III in Fig. 4. A tetracritical point exists at $\lambda=1$, at which transition lines for 2θ and 4θ orderings cross. The setting angle of the HB phase is constant in phases I and II, but varies with temperature and λ in phase III. We have found that there are two degenerate states of setting angle in the 2-4 model, which are related by a reflection about $y=45°$ line. This degeneracy does not reflect a symmetry of the system and is resolved by the dipole interaction. For the 2-1 model, which includes quadrupole and dipole interactions, we also have four phases in the T-λ plane. In phases I and II the setting angle is constant, but it increases as the temperature is reduced in phase III. By varying the ratio of the dipole to the quadrupole interactions λ and the strength of the anisotropic term β, and also varying the crystal field V_3, we can obtain various forms of the setting angle as a function of the temperature. We have calculated the spin-wave spectrum of rotors for the 2-4 model and found a gap at the spectrum provided that the interaction parameters do not exceed critical values, which confirms the stability of HB phase.

Crucial information that can guide us in sorting out appropriate terms are the observation that the HB phase makes a 55° angle with respect to the [100] direction and the smallness of the crystal-field anisotropy. For a model with quadrupole interaction and crystal-field anisotropy, the magnitude of V_3 of the lattice anisotropy should be rather big to produce the 55° HB phase, which is not likely, as discussed in Sec. III B. A reservation we have with the 2-4 model for describing the interchain orientational ordering of $(CH)_x$ is the fact that there is a twofold degeneracy of the setting angle. If this is a true symmetry of the system, we should be able to observe the 35° HB phase as well as the 55° one. Even though an anisotropic crystal field resolves this degeneracy, the difference between these two states will be small because of the smallness of V_3, which implies that the 35° HB phase should be observable. The 2-1 model with small anisotropy seems to be the best effective Hamiltonian with which to explain the experimental observations. In order to estimate the interaction parameters, we need more experimental data, especially the temperature dependence of the setting angle of the HB phase. Determination of the phonon or spin-wave spectrum will also be very fruitful. In our calculation, the energy scale is set by parameter α, which we have not calculated from a more microscopic theory. If α is too big, or the critical temperature is too high, then the $(CH)_x$ sample will become unstable before we reach the critical region. On the other hand, if α is too small, one has to be able to measure the setting angle with very good resolution.

We are currently studying the dopant ordering in the process of alkali doping of $(CH)_x$, assuming that the angular displacements are the soft degrees of freedom compared with the density ones. This has not been firmly established yet. For dopants bigger than the lattice distance, because of rather strong perturbation caused by their size, there will be translational deformation as well as the orientational ones. In fact, it was proposed by several groups that potassium-doped $(CH)_x$ has a tetragonal structure.[15] It will be very interesting and fruitful to consider both the density modulations and the angular displacements, and the interplay between them.

APPENDIX A: LANDAU THEORY FOR THE 2-4 MODEL

In this Appendix we present some specific calculations with the Landau expansion for the 2-4 model, the orientational energy of which is given by Eq. (5′). By expanding the free energy in terms of the order parameters up to fourth order, we will be able to determine (a) whether the transition becomes discontinuous, (b) whether the pinwheel phase, which is the equal condensation of three orientations of HB phase, exists, and (c) whether the same orientation is favored between HB phases associated with quadrupole and octopole interactions. We will also find the asymptotic forms of the order parameters near the phase boundaries, with our attention focused on the tetracritical point $\lambda=1$ where the transition lines for the 2θ and 4θ ordering cross. To do this we will take a density matrix of the following form:

$$\rho_i(\theta_i)=\frac{1}{2\pi}\left[1+\sum_{m=1}^{\infty} C_i(m)\cos(2m\theta_i) + S_i(m)\sin(2m\theta_i)\right]. \tag{A1}$$

Note the change by the factor of 2 from Eq. (11). General expression for the quadratic terms of the free energy is given by Eqs. (20) and (22). So we substitute

$$A_{ij}^{(2,2)}=\alpha+\beta,\quad B_{ij}^{(2,2)}=\beta,\quad A_{ij}^{(4,4)}=\lambda(\alpha+\beta),\quad B_{ij}^{(4,4)}=\lambda\beta,\quad A_{ij}^{(l,m)}=B_{ij}^{(l,m)}=0 \tag{A2}$$

[for other (l,m)], into Eq. (22) to obtain the quadratic terms of the free energy of the 2-4 model. We find

$$\Gamma'^{(cc)}_{1,1}(\mathbf{q})=\tfrac{1}{2}T+\tfrac{1}{2}\alpha(\gamma_1+\gamma_2+\gamma_3)+\tfrac{1}{2}\beta(\gamma_1+\tfrac{1}{4}\gamma_2+\tfrac{1}{4}\gamma_3)\ , \tag{A3a}$$

$$\Gamma'^{(cc)}_{2,2}(\mathbf{q})=\tfrac{1}{2}T+\tfrac{1}{2}\alpha_4(\gamma_1+\gamma_2+\gamma_3)+\tfrac{1}{2}\beta_4(\gamma_1+\tfrac{1}{4}\gamma_2+\tfrac{1}{4}\gamma_3)\ , \tag{A3b}$$

$$\Gamma'^{(cs)}_{1,1}(\mathbf{q})=\Gamma'^{(sc)}_{1,1}(\mathbf{q})=\tfrac{1}{8}\beta\sqrt{3}(\gamma_2-\gamma_3)\ , \tag{A3c}$$

$$\Gamma'^{(cs)}_{2,2}(\mathbf{q})=\Gamma'^{(sc)}_{2,2}(\mathbf{q})=-\tfrac{1}{8}\beta_4\sqrt{3}(\gamma_2-\gamma_3)\ , \tag{A3d}$$

$$\Gamma'^{(ss)}_{1,1}(\mathbf{q})=\tfrac{1}{2}T+\tfrac{1}{2}\alpha(\gamma_1+\gamma_2+\gamma_3)+\tfrac{3}{8}\beta(\gamma_2+\gamma_3)\ , \tag{A3e}$$

$$\Gamma'^{(ss)}_{2,2}(\mathbf{q})=\tfrac{1}{2}T+\tfrac{1}{2}\alpha_4(\gamma_1+\gamma_2+\gamma_3)+\tfrac{3}{8}\beta_4(\gamma_2+\gamma_3)\ , \tag{A3f}$$

where $\gamma_i=\cos(\mathbf{q}\cdot\boldsymbol{\delta}_i)$, where $\boldsymbol{\delta}_i$ is the ith-nearest-neighbor vector: $\boldsymbol{\delta}_1=a\hat{\mathbf{j}}$, $\boldsymbol{\delta}_2=\frac{1}{2}a(\sqrt{3}\hat{\mathbf{i}}+\hat{\mathbf{j}})$, and $\boldsymbol{\delta}_3=\frac{1}{2}a(\sqrt{3}\hat{\mathbf{i}}-\hat{\mathbf{j}})$. Because of the change in our definition by the factor of 2, $\Gamma'_{m,m}$ of Eqs. (A3) corresponds to $\Gamma_{2m,2m}$ of Eqs. (20) and (22). To obtain the fourth-order terms in the Landau expansion, we need to extend the expansion in Eqs. (18) to higher order. Considering a density matrix of Eq. (A1) with terms up to $m=4$, we find the third-order contribution, $\Delta F^{(3)}$, to the free energy per rotor to be

$$\Delta F^{(3)}=-\frac{T}{8N}\sum_i (C_i(2)\{[C_i(1)]^2-[S_i(1)]^2\}+2S_i(2)C_i(1)S_i(1)+2C_i(3)[C_i(2)C_i(1)-S_i(2)S_i(1)]$$
$$+2S_i(3)[C_i(2)S_i(1)+S_i(2)C_i(1)]+C_i(4)\{[C_i(2)]^2-[S_i(2)]^2\}+2S_i(4)C_i(2)S_i(2))\ . \tag{A4}$$

In writing this equation we only kept terms involving two order parameters which are critical, i.e., $Q(1)$ and $Q(2)$, where Q denotes a C_i or an S_i. [Below we use $Q(3)$ to denote $C_i(3)$ or $S_i(3)$.] Likewise the fourth-order contribution to the free energy, $\Delta F^{(4)}$, is

$$\Delta F^{(4)}=\frac{T}{32N}\sum_i (\{[C_i(1)]^2+[S_i(1)]^2\}^2+4\{[C_i(1)]^2+[S_i(1)]^2\}\{[C_i(2)]^2+[S_i(2)]^2\}+\{[C_i(2)]^2+[S_i(2)]^2\}^2)\ . \tag{A5}$$

Now we introduce normal modes by

$$x_A=S_1(\mathbf{Q}_A),\quad y_A=C_1(\mathbf{Q}_A)\ , \tag{A6a}$$

$$x_B=-\tfrac{1}{2}[\sqrt{3}C_1(\mathbf{Q}_B)+S_1(\mathbf{Q}_B)],\quad y_B=\tfrac{1}{2}[C_1(\mathbf{Q}_B)-\sqrt{3}S_1(\mathbf{Q}_B)]\ , \tag{A6b}$$

$$\sigma_A=S_2(\mathbf{Q}_A),\quad \eta_A=C_2(\mathbf{Q}_A)\ , \tag{A6c}$$

$$\sigma_B=\tfrac{1}{2}[\sqrt{3}C_2(\mathbf{Q}_B)-S_2(\mathbf{Q}_B)],\quad \eta_B=\tfrac{1}{2}[C_2(\mathbf{Q}_B)+\sqrt{3}S_2(\mathbf{Q}_B)]\ , \tag{A6d}$$

and so forth for the other wave vectors. The quadratic form of the free energy per rotor is diagonal in terms of these new coordinates:

$$F=\tfrac{1}{4}(T-T_{c,2})(x_A^2+x_B^2+x_C^2)+\tfrac{1}{4}(T-T_{c,4})(\sigma_A^2+\sigma_B^2+\sigma_C^2)+\tfrac{1}{4}(T+T_y)(y_A^2+y_B^2+y_C^2)$$
$$+\tfrac{1}{4}(T+T_\eta)(\eta_A^2+\eta_B^2+\eta_C^2)+\tfrac{1}{4}(T+T_{2,0})\{[C_1(\mathbf{q}=\mathbf{0})]^2+[S_1(\mathbf{q}=\mathbf{0})]^2\}$$
$$+\tfrac{1}{4}(T+T_{4,0})\{[C_2(\mathbf{q}=\mathbf{0})]^2+[S_2(\mathbf{q}=\mathbf{0})]^2\}+\tfrac{1}{4}T\sum_i\{[S_i(3)]^2+[C_i(3)]^2+[S_i(4)]^2+[C_i(4)]^2\}\ , \tag{A7}$$

where $T_{c,2}=\alpha+(3\beta/2)$, $T_{c,4}=\alpha_4+\frac{3}{2}\beta_4$, $T_y=\frac{1}{2}\beta-\alpha$, $T_\eta=\frac{1}{2}\beta_4-\alpha_4$, $T_{2,0}=3\alpha+(3\beta/2)$, and $T_{4,0}=3\alpha_4+\frac{3}{2}\beta_4$. Note that $Q(3)$ and $Q(4)$ have only entropic contributions and hence are already diagonal. For zero wave vector and for other m values in Eqs. (A1) the free energy is already diagonal, so that new coordinates do not need to be introduced. Since we need only consider coupling within the manifold of these $\mathbf{q}$'s, we write

$$C_i(1)=y_A e^{i\mathbf{Q}_A\cdot\mathbf{r}_i}+\tfrac{1}{2}(-\sqrt{3}x_B+y_B)e^{i\mathbf{Q}_B\cdot\mathbf{r}_i}+\tfrac{1}{2}(\sqrt{3}x_C+y_C)e^{i\mathbf{Q}_C\cdot\mathbf{r}_i}+C_1(\mathbf{q}=\mathbf{0})\ , \tag{A8a}$$

$$S_i(1)=x_A e^{i\mathbf{Q}_A\cdot\mathbf{r}_i}-\tfrac{1}{2}(x_B+\sqrt{3}y_B)e^{i\mathbf{Q}_B\cdot\mathbf{r}_i}+\tfrac{1}{2}(-x_C+\sqrt{3}y_C)e^{i\mathbf{Q}_C\cdot\mathbf{r}_i}+S_1(\mathbf{q}=\mathbf{0})\ , \tag{A8b}$$

$$C_i(2)=\eta_A e^{i\mathbf{Q}_A\cdot\mathbf{r}_i}+\tfrac{1}{2}(\sqrt{3}\sigma_B+\eta_B)e^{i\mathbf{Q}_B\cdot\mathbf{r}_i}+\tfrac{1}{2}(-\sqrt{3}\sigma_C+\eta_C)e^{i\mathbf{Q}_C\cdot\mathbf{r}_i}+C_2(\mathbf{q}=\mathbf{0})\ , \tag{A8c}$$

$$S_i(2)=\sigma_A e^{i\mathbf{Q}_A\cdot\mathbf{r}_i}+\tfrac{1}{2}(-\sigma_B+\sqrt{3}\eta_B)e^{i\mathbf{Q}_B\cdot\mathbf{r}_i}-\tfrac{1}{2}(\sigma_C+\sqrt{3}\eta_C)e^{i\mathbf{Q}_C\cdot\mathbf{r}_i}+S_2(\mathbf{q}=\mathbf{0})\ . \tag{A8d}$$

The critical variables of interest to us are the x's and the σ's. For $\lambda<1$, $T_{c,2}>T_{c,4}$ and the x's become critical first as the temperature is reduced, whereas for $\lambda>1$, $T_{c,4}>T_{c,2}$ and the σ's become critical first. In $\Delta F^{(4)}$ we keep only the terms involving only the x's and the σ's. Using Eqs. (A8) in Eq. (A5), we find that

$$\Delta F^{(4)}=\tfrac{1}{32}T[X^4+\Sigma^4+4\Sigma^2X^2+2(\boldsymbol{\Sigma}\cdot\mathbf{X})^2-2\sigma_A^2x_A^2-2\sigma_B^2x_B^2-2\sigma_C^2x_C^2+\sigma_A^2\sigma_B^2+\sigma_A^2\sigma_C^2+\sigma_B^2\sigma_C^2+x_A^2x_B^2+x_A^2x_C^2+x_B^2x_C^2]\ , \tag{A9}$$

where $\mathbf{X}$ denotes the three-component vector (x_A,x_B,x_C) and $\mathbf{\Sigma}(\sigma_A,\sigma_B,\sigma_C)$. The fourth-order terms in Eq. (A9) have a symmetry reminiscent of two coupled three-component Heisenberg models with a type of cubic anisotropy. We introduce the notation

$$X_{4c}=x_A^2x_B^2+x_B^2x_C^2+x_A^2x_C^2 , \tag{A10a}$$

$$\Sigma_{4c}=\sigma_A^2\sigma_B^2+\sigma_B^2\sigma_C^2+\sigma_A^2\sigma_C^2 , \tag{A10b}$$

$$(\mathbf{\Sigma}\cdot\mathbf{X})_{4c}^2=x_A^2\sigma_A^2+x_B^2\sigma_B^2+x_C^2\sigma_C^2 , \tag{A10c}$$

so that

$$\Delta F^{(4)}=\tfrac{1}{32}T[X^4+\Sigma^4+4\Sigma^2X^2+2(\mathbf{\Sigma}\cdot\mathbf{X})^2+\Sigma_{4c}+X_{4c}-2(\mathbf{\Sigma}\cdot\mathbf{X})_{4c}^2] . \tag{A9'}$$

In $\Delta F^{(3)}$ we need to keep terms which are linear or quadratic in the critical variables, the x's and the σ's. We find that

$$\begin{aligned}\Delta F^{(3)}=&-\tfrac{1}{8}T[2\eta_Ax_Bx_C+2\eta_Bx_Ax_C+2\eta_Cx_Ax_B+C_2(\mathbf{q}=\mathbf{0})(-x_A^2+\tfrac{1}{2}x_B^2+\tfrac{1}{2}x_C^2)+\tfrac{1}{2}\sqrt{3}S_2(\mathbf{q}=\mathbf{0})(x_B^2-x_C^2)\\&+C_1(\mathbf{q}=\mathbf{0})(2x_A\sigma_A-x_B\sigma_B-x_C\sigma_C)+S_1(\mathbf{q}=\mathbf{0})\sqrt{3}(\sigma_Cx_C-\sigma_Bx_B)+2y_A(\sigma_Bx_C+x_B\sigma_C)\\&-2y_B(\sigma_Ax_C+x_A\sigma_C)+2y_C(\sigma_Ax_B+x_A\sigma_B)-2C_3(\mathbf{q}=\mathbf{0})\mathbf{\Sigma}\cdot\mathbf{X}+C_3(\mathbf{Q}_A)e^{i\mathbf{Q}_A\cdot\mathbf{r}_i}(x_B\sigma_C+x_C\sigma_B)\\&+C_3(\mathbf{Q}_B)e^{i\mathbf{Q}_B\cdot\mathbf{r}_i}(x_A\sigma_C+x_C\sigma_A)+C_3(\mathbf{Q}_C)e^{i\mathbf{Q}_C\cdot\mathbf{r}_i}(x_A\sigma_B+x_B\sigma_A)+\sqrt{3}S_3(\mathbf{Q}_A)(x_B\sigma_C-x_C\sigma_B)\\&+\sqrt{3}S_3(\mathbf{Q}_B)(x_C\sigma_A-x_A\sigma_C)+\sqrt{3}S_3(\mathbf{Q}_C)(x_A\sigma_B-x_B\sigma_A)+C_4(\mathbf{q}=\mathbf{0})(-\sigma_A^2+\tfrac{1}{2}\sigma_B^2+\tfrac{1}{2}\sigma_C^2)\\&-2\sigma_B\sigma_CC_4(\mathbf{Q}_A)+\sigma_A\sigma_CC_4(\mathbf{Q}_B)+\sigma_A\sigma_BC_4(\mathbf{Q}_C)+\tfrac{1}{2}\sqrt{3}S_4(\mathbf{q}=\mathbf{0})(\sigma_C^2-\sigma_B^2)\\&+\sqrt{3}\sigma_A\sigma_BS_4(\mathbf{Q}_C)-\sqrt{3}\sigma_A\sigma_CS_4(\mathbf{Q}_B)] .\end{aligned} \tag{A11}$$

Now we eliminate the noncritical variables from Eq. (A11), using Eq. (A7). Thus, for example, we find that

$$C_2(\mathbf{q}=\mathbf{0})=-\tfrac{1}{4}(x_A^2-\tfrac{1}{2}x_B^2-\tfrac{1}{2}x_C^2)\frac{T}{T+T_{4,0}} , \tag{A12a}$$

$$S_2(\mathbf{q}=\mathbf{0})=\tfrac{1}{8}\sqrt{3}(x_B^2-x_C^2)\frac{T}{T+T_{4,0}} , \tag{A12b}$$

$$C_4(\mathbf{q}=\mathbf{0})=-\tfrac{1}{4}(\sigma_A^2-\tfrac{1}{2}\sigma_B^2-\tfrac{1}{2}\sigma_C^2) , \tag{A12c}$$

$$S_4(\mathbf{q}=\mathbf{0})=\tfrac{1}{4}\sqrt{3}(\sigma_C^2-\sigma_B^2) , \tag{A12d}$$

$$S_1(\mathbf{q}=\mathbf{0})=\tfrac{1}{4}\sqrt{3}(x_C\sigma_C-x_B\sigma_B)\frac{T}{T+T_{2,0}} , \tag{A12e}$$

$$C_1(\mathbf{q}=\mathbf{0})=\tfrac{1}{4}(2x_A\sigma_A-x_B\sigma_B-x_C\sigma_C)\frac{T}{T+T_{2,0}} . \tag{A12f}$$

We do not give results for those noncritical variables, which are only induced by simultaneous fluctuations at two different wave vectors, since these would only come into play in the pinwheel phase, whose existence is unlikely. When this procedure is carried out, the terms in Eq. (A11) give rise to additional contributions of quartic order, namely

$$\begin{aligned}\Delta F^{(3)}=&-\tfrac{1}{64}T^2\{4X_{4c}(T+T_\eta)^{-1}+(X^4-3X_{4c})(T+T_{4,0})^{-1}+[6(\mathbf{\Sigma}\cdot\mathbf{X})_c^2-2(\mathbf{\Sigma}\cdot\mathbf{X})^2](T+T_{2,0})^{-1}\\&+[4\Sigma^2X^2+2(\mathbf{\Sigma}\cdot\mathbf{X})^2-6(\mathbf{\Sigma}\cdot\mathbf{X})_c^2](T+T_y)^{-1}+[2(\mathbf{\Sigma}\cdot\mathbf{X})^2+4\Sigma^2X^2+\Sigma^4+\Sigma_{4c}-2(\mathbf{\Sigma}\cdot\mathbf{X})_c^2]T^{-1}\} .\end{aligned} \tag{A13}$$

Thus, in all, the free energy per rotor due to fluctuations at the herringbone wave vectors is

$$\begin{aligned}F=&\tfrac{1}{4}(T-T_{c,2})(x_A^2+x_B^2+x_C^2)+\tfrac{1}{4}[T-T_{c,4}(\alpha)](\sigma_A^2+\sigma_B^2+\sigma_C^2)\\&+\tfrac{1}{8}T[u_\sigma\Sigma^4+u_xX^4+u_{\sigma,x}\Sigma^2X^2+v(\mathbf{\Sigma}\cdot\mathbf{X})^2+v_{4c,x}X_{4c}+v_{4c,\sigma}\Sigma_{4c}+v_{4c,x\sigma}(\mathbf{\Sigma}\cdot\mathbf{X})_c^2] .\end{aligned} \tag{A14}$$

In Eq. (A14) the coefficients are

$$u_\sigma = \tfrac{1}{8} , \tag{A15a}$$

$$u_x = \frac{1}{4} - \frac{1}{8}\frac{T}{T+T_{4,0}} , \tag{A15b}$$

$$u_{\sigma,x} = \frac{1}{2} - \frac{1}{2}\frac{T}{T+T_y} , \tag{A15c}$$

$$v = \frac{1}{4} + \frac{1}{4}\frac{T}{T+T_{2,0}} - \frac{1}{4}\frac{T}{T+T_y} , \tag{A15d}$$

$$v_{4c,x} = \frac{1}{4} + \frac{3}{8}\frac{T}{T+T_{4,0}} - \frac{1}{2}\frac{T}{T+T_\eta} , \tag{A15e}$$

$$v_{4c,\sigma} = \tfrac{1}{8} , \tag{A15f}$$

$$v_{4c,x\sigma} = -\frac{1}{4} - \frac{3}{4}\frac{T}{T+T_{2,0}} + \frac{3}{4}\frac{T}{T+T_y} . \tag{A15g}$$

From these results we can determine (a) whether the transition becomes discontinuous, (b) whether the pinwheel phase exists, and (c) whether the same orientation is favored between HB phases associated with quadrupole and octopole interactions. For the pinwheel phase to exist, the anisotropy would have to be such as to favor simultaneous condensation of three wave vectors. This would require $v_{4c,x}$ to be negative. Although this is not impossible, it seems to require rather extreme values of the parameters. In fact, we see that fluctuations are unlikely to modify the signs of the various fourth-order coefficients listed in Eqs. (A15). Thus, we expect that the transition will normally be continuous. For the same orientation to be favored, it is required that $v + v_{4c,x\sigma} < 0$. Near the transition temperature, this condition is reduced to $4\alpha + \beta < 0$. Thus for $\alpha = -1$, the same orientation is favored when $\beta < 4$. We can also use these results to find the asymptotic forms for the order parameters near the various phase boundaries. For this purpose we reduce the number of parameters by setting $\alpha_4 = \lambda\alpha$ and $\beta_4 = \lambda\beta$, in which case we consider the phase diagram as a function of λ as shown in Fig. 4 and our attention is focused on the tetracritical point at $\lambda = 1$, where the transition lines for 2θ and 4θ ordering cross. We will consider the various cases where these lines are approached as the temperature is increased for λ either less than or greater than unity.

For concreteness we consider condensation into a herringbone state with modulation vector $\mathbf{Q}_A$. Then the critical fluctuations at wave vector $\mathbf{Q}_A$ involve $\sin 2\theta$, as described by the variable x_A, and $\sin 4\theta$, as described by the variable σ_A. The noncritical variables will keep track of the described fluctuations at zero wave vector and involve $\cos 2\theta$, as described by the variable $C_1(\mathbf{q}=\mathbf{0})$, and $\cos 4\theta$, as described by the variable $C_2(\mathbf{q}=\mathbf{0})$. Without consideration of the fourth-order terms in the free energy, one has criticality of x_A at $T_{c,2}$, which is independent of λ, and criticality of σ_A at $T_{c,4}(\lambda)$ given by

$$T_{c,4}(\lambda) = \lambda T_{c,2} . \tag{A16}$$

For case I, $T \to T_{c,2}$ with $\lambda < 1$, we have

$$x_A = \left[\frac{T_{c,2} - T}{u_x T_{c,2}} \right]^{1/2} \tag{A17}$$

and, using Eq. (A12),

$$C_2(\mathbf{q}=\mathbf{0}) = -\frac{1}{4}\frac{T_{c,2} - T}{u_x (T + T_{4,0})} . \tag{A18}$$

For case II, $T \to T_{4,c}(\lambda)$ with $\lambda > 1$, we have

$$\sigma_A = \left[\frac{T_{c,4}(\lambda) - T}{u_\sigma T_{c,4}(\lambda)} \right]^{1/2} . \tag{A19}$$

To obtain the asymptotic behavior in the intermediate phase we specialize Eq. (A7) to the case of a single modulation vector $\mathbf{Q}_A$:

$$F = \tfrac{1}{4}(T - T_{c,2})x^2 + \tfrac{1}{4}[T - T^{(0)}_{c,4}(\lambda)]\sigma^2 + \frac{T}{8}[u_\sigma \sigma^4 + u_x x^4 + (u_{\sigma,x} + v + v_{4c,x\sigma})x^2\sigma^2] , \tag{A20}$$

where $T^{(0)}_{c,4}(\lambda)$ denotes the "bare" value of the transition temperature: $T^{(0)}_{c,4}(\lambda) = \lambda T_{c,2}$. As we shall see, the actual transition occurs at a renormalized transition temperature which we denote $T_{c,4}(\lambda)$.

We now consider case III: $T \to T_{c,4}(\lambda)$ with $\lambda < 1$. We therefore minimize F with respect to x to find

$$F = \tfrac{1}{8}\sigma^4 T \left[u_\sigma - \frac{\beta^2}{u_x} \right] + \tfrac{1}{4}\sigma^2 \left[T\left[1 - \frac{\beta}{u_x} \right] - \left[T^{(0)}_{c,4}(\lambda) - T_{c,2}\frac{\beta}{u_x} \right] \right] , \tag{A21}$$

where

$$\beta = \tfrac{1}{2}(u_{\sigma,x} + v + v_{4c,x\sigma}) = \frac{1}{4}\frac{T_{2,0}}{T + T_{2,0}} . \tag{A22}$$

From Eq. (A21) we obtain the results

$$\frac{dT_{c,4}(\lambda)}{d\lambda} = \frac{dT^{(0)}_{c,4}(\lambda)}{d\lambda}\frac{1}{1 - \beta/u_x} = \frac{T_{c,2}}{1 - \beta/u_x} , \tag{A23}$$

$$\sigma^2 = \frac{T_{c,4}(\lambda) - T}{u_\sigma T}\frac{1 - \beta/u_x}{1 - \beta^2/(u_x u_\sigma)} . \tag{A24}$$

We have assumed that λ is close to unity, in which case Eq. (A19) continues to hold and Eqs. (A18) have approximate validity. Also, from Eq. (A12f) we see that

$$C_1(\mathbf{q}=\mathbf{0}) = \tfrac{1}{2}x_A \sigma_A \frac{T}{T + T_{2,0}} = \tfrac{1}{2}x_A \left[\frac{T_{c,4}(\lambda) - T}{u_\sigma T_{c,4}(\lambda)} \right]^{1/2} \frac{T}{T + T_{2,0}} . \tag{A25}$$

Finally, for case IV, $T \to T_{c,2}(\lambda)$ with $\lambda > 1$, we find the renormalized slope of the phase boundary by calculations analogous to those for case III. Minimizing F with respect to σ, we obtain

$$F=\frac{T}{8}x^4\left[u_x-\frac{\beta^2}{u_\sigma}\right]+\tfrac{1}{4}x^2\left[T\left[1-\frac{\beta}{u_\sigma}\right]-\left[T_{c,2}-\frac{\beta T_{c,4}^{(0)}(\lambda)}{u_\sigma}\right]\right]. \quad \text{(A26)}$$

We thereby find that

$$\frac{dT_{c,2}(\lambda)}{d\lambda}=-\frac{dT_{c,4}(\lambda)}{d\lambda}\frac{\beta/u_\sigma}{1-\beta/u_\sigma}=-\frac{T_{c,2}\beta/u_\sigma}{1-\beta/u_\sigma} \quad \text{(A27)}$$

and

$$x^2=\frac{T_{c,2}(\lambda)-T}{u_x T}\frac{1-\beta/u_\sigma}{1-\beta^2/u_x u_\sigma}. \quad \text{(A28)}$$

We also find from Eq. (A12f) that

$$C_1(\mathbf{q}=\mathbf{0})=\tfrac{1}{2}\sigma_A x_A\frac{T}{T+T_{2,0}}=\tfrac{1}{2}\sigma_A\left[\frac{T_{c,2}(\lambda)-T}{u_x T_{c,2}(\lambda)}\right]^{1/2}\frac{T}{T+T_{2,0}}. \quad \text{(A29)}$$

These results are compared with numerical work, and agree within a few percent of their numerically determined counterparts.

APPENDIX B: LANDAU THEORY FOR THE $\sqrt{3}\times\sqrt{3}$ PHASE

Now we carry out some analyses for the ordering transition of the $\sqrt{3}\times\sqrt{3}$ phase found in Sec. III A. For this phase there are two inequivalent $\mathbf{Q}_{\sqrt{3}}$'s, which we will denote as $\mathbf{Q}_{\sqrt{3}}$ and $-\mathbf{Q}_{\sqrt{3}}$ with

$$\mathbf{Q}_{\sqrt{3}}=\hat{\mathbf{j}}4\pi/(3a). \quad \text{(B1)}$$

In this case $\mathbf{Q}_{\sqrt{3}}$ and $-\mathbf{Q}_{\sqrt{3}}$ are not equivalent because $3\mathbf{Q}_{\sqrt{3}}$ is equal to reciprocal-lattice vector: $3\mathbf{Q}_{\sqrt{3}}=2\mathbf{G}_1+\mathbf{G}_2$ in the notation of Eq. (8). As in the calculations leading to Eq. (A14), we focus here on fluctuations induced by $\sqrt{3}$ fluctuations at the wave vectors $\mathbf{Q}_{\sqrt{3}}$ and $-\mathbf{Q}_{\sqrt{3}}$. We set

$$C_1(\mathbf{Q}_{\sqrt{3}})=Ce^{i\chi},\quad S_1(\mathbf{Q}_{\sqrt{3}})=Se^{i\psi}. \quad \text{(B2)}$$

Note the inverse of Eq. (19):

$$C_i(1)=\sum_{\mathbf{Q}_{\sqrt{3}}}C_1(\mathbf{Q}_{\sqrt{3}})e^{-i\mathbf{Q}_{\sqrt{3}}\cdot\mathbf{r}_i}. \quad \text{(B3)}$$

Thus for the a, b, and c sublattices we have, respectively,

$$C_a(1)=2C\cos\chi,\quad S_a(1)=2S\cos\psi, \quad \text{(B4a)}$$

$$C_b(1)=2C\cos(\chi+120°),\quad S_b(1)=2S\cos(\psi+120°), \quad \text{(B4b)}$$

$$C_c(1)=2C\cos(\chi-120°),\quad S_c(1)=2S\cos(\psi-120°). \quad \text{(B4c)}$$

Using Eqs. (17) we find that the quadratic terms in the free energy per rotor are

$$F=\tfrac{1}{2}(T-T_{\sqrt{3}})(S^2+C^2)+\frac{T}{12}\sum_{\alpha=a,b,c}\{[C_\alpha(2)]^2+[S_\alpha(2)]^2\}. \quad \text{(B5)}$$

Here $C_\alpha(2)$ and $S_\alpha(2)$ denote the values of $C_i(2)$ and $S_i(2)$, respectively, when site i is in the α sublattice. We kept the terms involving $C_\alpha(2)$ and $S_\alpha(2)$ since the cubic terms in the free energy will involve these terms. The problem we now address is to what extent the higher-order anisotropies fix the phases ψ and χ. Since the contributions within mean-field theory which are higher order in powers of S and C are local, we find it convenient to tabulate the order parameters at sublattices a, b, and c, where $r_a=0$, $r_b=\delta_1$, and $r_c=\delta_2$ are the representatives of the three sublattices of the $\sqrt{3}$ structure. Using Eq. (A4) we find the third-order contribution to the free energy per rotor to be

$$\Delta F^{(3)}=-\frac{T}{6}\sum_\alpha\{C_\alpha(2)[C^2\cos^2(\chi-\epsilon_\alpha)-S^2\cos^2(\psi-\epsilon_\alpha)]+2S_a(2)CS\cos(\chi-\epsilon_\alpha)\cos(\psi-\epsilon_\alpha)\}, \quad \text{(B6)}$$

where the sum is over sublattices α with $\epsilon_a=0$, $\epsilon_b=-120°$, and $\epsilon_c=120°$. Similarly, using Eq. (A5) we obtain the fourth-order contribution to the free energy per rotor as

$$\Delta F^{(4)}=\frac{T}{6}\sum_\alpha\{[C^2\cos^2(\chi-\epsilon_\alpha)+S^2\cos^2(\psi-\epsilon_\alpha)]^2\}. \quad \text{(B7)}$$

We now minimize the free energy with respect to $C_\alpha(2)$ and $S_\alpha(2)$. Thereby we obtain the contribution induced in the fourth-order term by $\Delta F^{(3)}$ as

$$\Delta F^{(3)}=-\frac{T}{12}\sum_\alpha\{[C^2\cos^2(\chi-\epsilon_\alpha)+S^2\cos^2(\psi-\epsilon_\alpha)]^2\}. \quad \text{(B8)}$$

Now we carry out the sums over ϵ:

$$\tfrac{1}{3}\sum_\alpha\cos^4(\chi-\epsilon_\alpha)=\tfrac{3}{8}, \quad \text{(B9a)}$$

$$\tfrac{1}{3}\sum_\alpha\cos^2(\chi-\epsilon_\alpha)\cos^2(\psi-\epsilon_\alpha)=\tfrac{1}{8}[3-2\sin^2(\chi-\psi)]. \quad \text{(B9b)}$$

Using these averages and combining Eqs. (B7) and (B8), we get the total free energy per rotor in terms of the order parameters C and S as

$$F=\tfrac{1}{2}(T-T_{\sqrt{3}})(S^2+C^2)+\frac{T}{32}[3(C^2+S^2)^2-4C^2S^2\sin^2(\chi-\psi)]. \quad \text{(B10)}$$

We now see the effect of the fourth-order anisotropy proportional to $C^2S^2\sin^2(\chi-\psi)$. To maximize this term for a given quadratic contribution requires having $S=C$ and $\chi=\psi\pm\pi/2$. So we see that

$$C_a(1)+iS_a(1)=2Ce^{i\chi}\,, \tag{B11a}$$

$$C_b(1)+iS_b(1)=2Ce^{i(\chi-2\pi\tau/3)}\,, \tag{B11b}$$

$$C_c(1)+iS_c(1)=2Ce^{i(\chi-4\pi/3)}\,, \tag{B11c}$$

where $\tau=+1$ corresponds to $\psi=\chi+\pi/2$ and $\tau=-1$ to $\psi=\chi-\pi/2$. So the fourth-order anisotropy leaves us with a model having a continuous phase symmetry in the parameter χ in a direct product with an Ising variable, τ. Presumably the effect of sixth-order anisotropy in a more general model will lead to a free-energy anisotropy of the form $V_3\cos(6\chi)$. We have not investigated the universality class of this.

We can investigate the nature of the $\sqrt{3}$ phase. From Eq. (B11) we can see how the rotor orientations vary as we go around the plaquette *a-b-c*. The angles vary as $\frac{1}{2}\chi$, $\frac{1}{2}-\tau 60°$, and $\frac{1}{2}\chi-\tau 120°$, where the Ising-like variable $\tau=\pm1$ indicates the sense of chirality. Next, one should look at the sixth-order anisotropy to see what orientations are favored. In fact, one can see that the mean-field free energy possesses an *exact invariance* with respect to global rotations. To see this, first note that the entropy is obviously invariant with respect to rotation of the local axes. Next, we ask about the energy. Clearly the term proportional to α is rotationally invariant. For the β term, note that in the $\sqrt{3}\times\sqrt{3}$ phase each molecule is surrounded by a shell of six nearest neighbors, three of which are on one sublattice and three of which are on another sublattice. We sum the energy over one subshell of three nearest neighbors. Let θ_0 be the orientations of the central rotor and θ be the orientation of its neighbor in the subshell along the x axis. Then the energy is

$$E=\beta[\cos(2\theta_0)\cos(2\theta)+\cos(2\theta_0+120°)\cos(2\theta+120°)+\cos(2\theta_0-120°)\cos(2\theta-120°)] \tag{B12a}$$

$$=\beta[\tfrac{3}{2}\cos(2\theta_0)\cos(2\theta)+\tfrac{3}{2}\sin(2\theta_0)\sin(2\theta)]=\tfrac{3}{2}\beta\cos(2\theta_0-2\theta)\,, \tag{B12b}$$

which shows that the energy depends only on the difference in angles of the rotors: it is invariant with respect to global rotation. This phase has the symmetry of the direct product of an x-y model with an Ising model (recall that the Ising variable gives the sense of chirality).[12]

It is easy to calculate the energies of the above phases at zero temperature. We find for each phase that the energy per rotor E is given by $E=-kT_c^{(0)}$, where $T_c^{(0)}$ is the approximate mean-field transition temperature given in Eq. (A26). There is no analogue of the modulated phase at zero temperature because the classical ground state should have fully aligned rotors: no longitudinal modulation of the order parameter is allowed. Thus we have the phase diagram shown in Fig. 2 for $\alpha=1$ in the β-T plane. All the order-disorder transitions are continuous, since there are no third-order terms in the free energy and the fourth-order terms are positive. The FM and $\sqrt{3}$ phases both have a continuous symmetry with respect to global rotations of all rotors. Hence, their excitation spectra are gapless. The excitation spectra of the HB phases have a gap. The modulation vector in the mod phase approaches smoothly the values appropriate for the $\sqrt{3}$ and HB phases as one approaches the respective phase boundaries. The nature of the transitions between the mod phases and the adjoining ordered phases is not completely obvious. At the Lifshitz point, the instabilities in $\cos2\theta$ and $\sin2\theta$ become degenerate. For larger values of β the transition temperature for the $\sin2\theta$ instability moves to higher temperature and the wave vector becomes incommensurate. However, the instability in $\cos2\theta$ is close by and must survive at lower temperature since the ground state is never modulated in such a longitudinal way. We think that the $\sqrt{3}$-mod transition must be discontinuous because rotors with a finite order parameter have to change their orientation at this transition. It is not clear without further study whether the mod-HB transition is or is not continuous.

APPENDIX C: INTERACTION BETWEEN THE ROTORS IN THE HB PHASE

We have calculated the spin-wave spectrum of rotors in the herringbone phase assuming a two-site unit cell in Sec. IV. The interactions between rotors in a unit cell and those in nearest-neighbor cells are given in Eq. (59). By studying the harmonic fluctuations around the minimum state of Eq. (59), we have obtained the spin-wave spectrum. In this appendix we will give the explicit expression for each term of Eq. (59). Recall that we set

$$\theta_{a,\mathbf{R}}=\theta_0+u_{a,\mathbf{R}},\quad \theta_{b,\mathbf{R}}=-\theta_0+u_{b,\mathbf{R}} \tag{60}$$

in order to expand the interaction up to the quadratic order in u's. Note that

$$\phi_{ij}=\pi/3,\quad \mathbf{r}_{ij}=\mathbf{r}(a,\mathbf{R})-\mathbf{r}(b,\mathbf{R})=-\mathbf{r}(a,\mathbf{R})+\mathbf{r}(b,\mathbf{R}-\mathbf{b}_2)\,, \tag{C1a}$$

$$\phi_{ij}=-\pi/3,\quad \mathbf{r}_{ij}=\mathbf{r}(a,\mathbf{R})-\mathbf{r}(b,\mathbf{R}-\mathbf{b}_1)=-\mathbf{r}(a,\mathbf{R})+\mathbf{r}(b,\mathbf{R}+\mathbf{b}_1-\mathbf{b}_2)\,, \tag{C1b}$$

$$\phi_{ij}=0,\quad \mathbf{r}_{ij}=\mathbf{r}(a,\mathbf{R})-\mathbf{r}(a,\mathbf{R}+\mathbf{b}_1)=-\mathbf{r}(b,\mathbf{R})+\mathbf{r}(b,\mathbf{R}+\mathbf{b}_1)\,. \tag{C1c}$$

Then, by substituting Eq. (C1) into Eq. (5), we get the following expressions for Eq. (59):

$$H(a,\mathbf{R};b,\mathbf{R}-\mathbf{b}_2)=\alpha\cos(2u_{a,\mathbf{R}}-2u_{b,\mathbf{R}-\mathbf{b}_2}+4\theta_0)+\alpha_4\cos(4u_{a,\mathbf{R}}-4u_{b,\mathbf{R}+\mathbf{b}_2}+8\theta_0)$$
$$+\beta\cos(2u_{a,\mathbf{R}}+2\theta_0-2\pi/3)\cos(2u_{b,\mathbf{R}-\mathbf{b}_2}-2\theta_0-2\pi/3)$$
$$+\beta_4\cos(4u_{a,\mathbf{R}}+4\theta_0+2\pi/3)\cos(4u_{b,\mathbf{R}-\mathbf{b}_2}-4\theta_0+2\pi/3)\ , \tag{C2a}$$

$$H(a,\mathbf{R};b,\mathbf{R}+\mathbf{b}_1-\mathbf{b}_2)=\alpha\cos(2u_{a,\mathbf{R}}-2u_{b,\mathbf{R}+\mathbf{b}_1-\mathbf{b}_2}+4\theta_0)+\alpha_4\cos(4u_{a,\mathbf{R}}-4u_{b,\mathbf{R}+\mathbf{b}_1-\mathbf{b}_2}+8\theta_0)$$
$$+\beta\cos(2u_{a,\mathbf{R}}+2\theta_0+2\pi/3)\cos(2u_{b,\mathbf{R}+\mathbf{b}_1-\mathbf{b}_2}-2\theta_0+2\pi/3)$$
$$+\beta_4\cos(4u_{a,\mathbf{R}}+4\theta_0-2\pi/3)\cos(4u_{b,\mathbf{R}+\mathbf{b}_1-\mathbf{b}_2}-4\theta_0-2\pi/3)\ , \tag{C2b}$$

$$H(a,\mathbf{R};a,\mathbf{R}+\mathbf{b}_1)=\alpha\cos(2u_{a,\mathbf{R}}-2u_{a,\mathbf{R}+\mathbf{b}_1})+\alpha_4\cos(4u_{a,\mathbf{R}}-4u_{a,\mathbf{R}+\mathbf{b}_1})$$
$$+\beta\cos(2u_{a,\mathbf{R}}+2\theta_0)\cos(2u_{a,\mathbf{R}+\mathbf{b}_1}+2\theta_0)+\beta_4\cos(4u_{a,\mathbf{R}}+4\theta_0)\cos(4u_{a,\mathbf{R}+\mathbf{b}_1}+4\theta_0)\ , \tag{C2c}$$

$$H(a,\mathbf{R};b,\mathbf{R})=\alpha\cos(2u_{a,\mathbf{R}}-2u_{b,\mathbf{R}}+4\theta_0)+\alpha_4\cos(4u_{a,\mathbf{R}}-4u_{b,\mathbf{R}}+8\theta_0)+\beta\cos(2u_{a,\mathbf{R}}+2\theta_0-2\pi/3)\cos(2u_{b,\mathbf{R}}-2\theta_0-2\pi/3)$$
$$+\beta_4\cos(4u_{a,\mathbf{R}}+4\theta_0+2\pi/3)\cos(4u_{b,\mathbf{R}}-4\theta_0+2\pi/3)\ , \tag{C2d}$$

$$H(a,\mathbf{R};b,\mathbf{R}-\mathbf{b}_1)=\alpha\cos(2u_{a,\mathbf{R}}-2u_{b,\mathbf{R}-\mathbf{b}_1}+4\theta_0)+\alpha_4\cos(4u_{a,\mathbf{R}}-4u_{b,\mathbf{R}-\mathbf{b}_1}+8\theta_0)$$
$$+\beta\cos(2u_{a,\mathbf{R}}+2\theta_0+2\pi/3)\cos(2u_{b,\mathbf{R}-b_1}-2\theta_0+2\pi/3)\ , \tag{C2e}$$

$$H(b,\mathbf{R};b,\mathbf{R}+\mathbf{b}_1)=\alpha\cos(2u_{b,\mathbf{R}}-2u_{b,\mathbf{R}+\mathbf{b}_1})+\alpha_4\cos(4u_{b,\mathbf{R}}-4u_{b,\mathbf{R}+\mathbf{b}_1})$$
$$+\beta\cos(2u_{b,\mathbf{R}}-2\theta_0)\cos(2u_{b,\mathbf{R}+\mathbf{b}_1}-2\theta_0)+\beta_4\cos(4u_{b,\mathbf{R}}-4\theta_0)\cos(4u_{b,\mathbf{R}+\mathbf{b}_1}-4\theta_0)\ . \tag{C2f}$$

By expanding Eqs. (C2) in powers of u's, Eqs. (62) and (66) follow.

[1] L. W. Shacklette and J. E. Toth, Phys. Rev. B **32**, 5892 (1985).

[2] M. Winokur, Y. B. Moon, A. J. Heeger, J. Barker, D. C. Bott, and H. Shirakawa, Phys. Rev. Lett. **58**, 2329 (1987).

[3] For general reviews, see S. Roth and H. Bleier, Adv. Phys. **36**, 385 (1987); A. J. Heeger, S. Kivelson, J. R. Schrieffer, and W. P. Su, Rev. Mod. Phys. **60**, 781 (1988).

[4] C. R. Fincher, Jr., C. E. Chen, A. J. Heeger, A. G. MacDiamid, and J. B. Hastings, Phys. Rev. Lett. **48**, 100 (1982).

[5] For a recent review, see S. A. Safran, in *Solid State Physics,* edited by H. Ehrenreich and D. Turnbull (Academic, New York, 1987), Vol. 40, p. 183.

[6] S. A. Safran, Phys. Rev. Lett. **44**, 937 (1980).

[7] J. Ma, H.-Y. Choi, E. J. Mele, and J. E. Fischer, Synth. Met. (to be published).

[8] H.-Y. Choi and E. J. Mele, Phys. Rev. B **40**, 3439 (1989).

[9] A. B. Harris, O. G. Mouritsen, and A. J. Berlinsky, Can. J. Phys. **62**, 915 (1984); A. B. Harris and A. J. Berlinsky, *ibid.* **57**, 1852 (1979).

[10] R. H. Baughman, N. S. Murth, G. G. Miller, L. W. Shacklette, and R. M. Metzger, J. Phys. (Paris) Colloq. **44**, C3-53 (1983).

[11] O. G. Mouritsen and A. J. Berlinsky, Phys. Rev. Lett. **48**, 181 (1982).

[12] D. H. Lee, J. D. Joannopoulos, J. W. Negele, and D. P. Landau, Phys. Rev. B **33**, 450 (1986); S. Miyashita and H. Shiba, J. Phys. Soc. Jpn. **53**, 1145 (1984).

[13] Two minima were obtained for *cis*-$(CH)_x$ from packing analysis at $\theta=51.7°$ and 33.8°, and the former is favored by a small amount of energy; see R. H. Baughman, S. L. Hsu, L. R. Anderson, G. P. Pez, and A. J. Signorelli, in *Molecular Metals,* edited by W. Hatfield (Plenum, New York, 1979), p. 189.

[14] D. H. Lee and G. Grinstein, Phys. Rev. Lett. **55**, 541 (1985); D. H. Lee, G. Grinstein, and J. Toner, *ibid.* **56**, 2318 (1986).

[15] R. H. Baughman, N. S. Murthy, and G. G. Miller, J. Chem. Phys. **79**, 515 (1983); R. H. Baughman, L. W. Shacklette, N. S. Murthy, G. G. Miller, and R. L. Elsenbaumer, Mol. Cryst. Liq. Cryst. **118**, 253 (1985); J. P. Pouget, in *Electronic Properties of Polymers and Related Compounds,* Vol. 63 of *Springer Series in Solid-State Sciences,* edited by H. Kuzmány, M. Mehring, and S. Roth (Springer-Verlag, Berlin, 1985), p. 26.